



UNIVERSITATEA POLITEHNICA DIN BUCUREȘTI

Școala Doctorală de Inginerie Electrică



PHD THESIS SUMMARY

Electromagnetic Interferences in the electric
systems of vehicles

Doctoral Student: Ing. Violeta-Maria Ionescu

Scientific Adviser: Prof. Dr. Ing. Mihai Octavian Popescu

Bucharest 2022

Table of contents

Chapter 1: Fundamentals		4
1.1.	<i>Introduction</i>	4
1.2.	<i>Objectives of the proposed theme</i>	5
1.3.	<i>Introductory notions about electromagnetic compatibility</i>	6
1.4.	<i>Brief history of electric vehicles</i>	7
1.5.	<i>Electromagnetic compatibility testing for electric vehicles</i>	7
Chapter 2: Structures of electric vehicles		8
2.1.	<i>Vehicle with electric battery (BEV)</i>	8
2.2.	<i>Hybrid electric vehicle (HEV)</i>	8
2.3.	<i>Hybrid plug-in vehicle (PHEV)</i>	9
2.4.	<i>Integration of the electrical / electronic system in electric vehicles</i>	9
Chapter 3: Significant electromagnetic field sources in electric vehicles		11
3.1.	<i>Static converter</i>	11
3.2.	<i>Electric motor</i>	11
3.3.	<i>Battery</i>	11
3.4.	<i>Shielded and unshielded cables</i>	11
3.5.	<i>Coupling mechanisms</i>	12
3.5.1.	<i>Galvanic coupling (conductive)</i>	12
3.5.2.	<i>Magnetic coupling (inductive)</i>	12
3.5.3.	<i>Electrical coupling (capacitive)</i>	12
3.5.4.	<i>Electromagnetic radiation coupling</i>	12
Chapter 4: Prevention and exposure regulations and standards		13
4.1.	<i>ICNIRP regulations</i>	13
4.2.	<i>Static magnetic field exposure regulations</i>	13
4.3.	<i>IEEE Exposure Standard</i>	12
4.4.	<i>Electromagnetic compatibility in the Automotive Industry</i>	14
4.5.	<i>UNECE Regulation 10</i>	17
4.6.	<i>CISPR Standard 25</i>	17
4.6.1.	<i>Antenna systems for CISPR 25</i>	17
4.6.2.	<i>Anechoic Room</i>	18
4.7.	<i>ISO 11452 Standard</i>	19
4.8.	<i>Possible victims of electromagnetic interference</i>	19
Chapter 5: Simulation of the magnetic field inside the electric vehicle		20
5.1.	<i>Simulation environment</i>	20
5.2.	<i>Geometry chosen for magnetic field simulation</i>	20
5.3.	<i>Cable track with return through the housing - asymmetrical construction</i>	21

5.4.	<i>Round trip cable route - Symmetrical construction</i>	21
5.5.	<i>Wire path with housing return - symmetrical construction</i>	22
5.6.	<i>Cable track with return by housing - symmetrical construction - 0 cm from the floor</i>	22
5.7.	<i>Cable track with return by housing - symmetrical construction - 10 cm from the floor</i>	23
5.8.	<i>Cable track with return by housing - symmetrical construction - 10 cm from the floor with seats</i>	24
5.9.	<i>Coaxial cable magnetic field simulation - asymmetric construction</i>	26
Chapter 6: Study of the interaction between the surrounding electromagnetic environment and the electric vehicle		27
6.1.	<i>Description of the ambient electromagnetic environment</i>	27
6.2.	<i>Analysis and simulation of the electromagnetic environment outside the electric vehicle</i>	27
6.3.	<i>Simulation of the magnetic field produced by a medium voltage power transfer line in the presence of a body car</i>	28
6.4.	<i>Analysis of the ambient electromagnetic environment inside the passenger compartment of the electric vehicle</i>	29
6.5.	<i>Electric and magnetic field measurement during charging of an electric vehicle</i>	30
6.5.1.	<i>Electric and magnetic field measurement for slow charging</i>	31
6.5.2.	<i>Electric and magnetic field measurement for fast charging</i>	33
Chapter 7: Electromagnetic field measurements of high voltage cables inside the body of electric vehicles		36
7.1.	<i>Installation used</i>	36
7.2.	<i>Case 1: Both cables are positioned side by side in the right corner of the body</i>	38
7.3.	<i>Case 2: Both cables are positioned side by side in the center of the body</i>	41
7.4.	<i>Case 3: Reverse cable - Symmetrical construction</i>	43
7.5.	<i>Case 4: One cable is positioned to the right and one to the center</i>	45
Chapter 8: Conclusions and own contributions		47
8.1.	<i>General conclusions</i>	47
8.2.	<i>Personal contributions</i>	49
8.3.	<i>Future directions of research</i>	50
List of published articles		51
Bibliography		52

Chapter 1: Fundamentals

1.1. Introduction

In the past years, electric and hybrid vehicles have become increasingly popular. This is primarily due to growing concerns about global carbon emissions as well as local exhaust emissions that make crowded cities highly polluted and unbearable to live in. Another important factor is declining global oil resources. While electric vehicles have not gained such popularity in the past due to technical limitations, design developments and improvements in rechargeable batteries, motors and controllers are an important factor in their development. ^[1]

The increasing complexity of the electrical and electronic systems of motor vehicles, together with the tightening of regulations related to fuel consumption and the emission of pollutants make it increasingly difficult to ensure electromagnetic compatibility between electrical and electronic systems mounted on the car.

Today's electronic systems contain far more active electronic components than in the past. As the emphasis is on fuel efficiency, electric and hybrid vehicles are gaining more and more popularity. These types of vehicles introduce new problems in terms of electromagnetic interference due to the high values of current. Internal electrical systems that may affect the operation of vehicles may include collision avoidance radar, radio navigation system, power steering system, autopilot, airbag inflator, wheel pressure sensor, etc.

In addition to the sources of electromagnetic interference of the systems mounted inside the cars, we also have the sources of external electromagnetic disturbances that can interfere with the electronic systems of vehicles. These external sources may include telecommunications systems, radio and TV transmissions, radar systems, power generation and transmission lines, electrical systems, automatic garage door openers, but also devices that are brought by passengers inside vehicles. such as bluetooth devices, mobile phone, video games.^[3]

Keywords: electromagnetic compatibility in the automotive industry, electromagnetic compatibility standards, electric vehicles, magnetic field experiments and simulations

1.2. Objectives of the proposed theme

It is estimated that by 2025, 30% of global vehicle sales will be electric and hybrid, making electromagnetic compatibility issues very important to ensure an operational electromagnetic environment.

In the case of electric vehicles, the passengers are very close to the vehicle's electrical system, which can have a significant impact. Relatively high currents flowing through the electrical system and short distances between power systems and passengers can cause significant exposure to the magnetic field. In this paper I will focus on the study of the magnetic field inside the passenger compartment of electric vehicles.

The theme of this doctoral dissertation is research and characterization of electromagnetic interference produced by automotive electrical systems. With the help of simulation methods, but also magnetic field measurement, the values of magnetic induction will be evaluated near the high voltage cables present in electric vehicles for various topologies and interactions with the environment.

In this paper we will focus on the following aspects:

- Brief history of vehicles;
- Description of the constructive structures of electric and hybrid vehicles;
- Analysis of significant magnetic field sources in electric vehicles;
- Identifying possible victims of electromagnetic interference;
- Classification of electromagnetic compatibility standards in the automotive industry;
- Simulation of the magnetic field inside the electric vehicle;
- Study and simulation of the interaction between the surrounding electromagnetic environment and the electric vehicle;
- Measurements of electromagnetic field produced by high voltage cables inside the body of electric vehicles;
- Comparison of the results obtained from the simulations with the measured values from the experiments on the magnetic field.

1.3. Introductory notions about electromagnetic compatibility

Electromagnetic compatibility is the ability of a device or system to operate in its electromagnetic environment, without affecting its functionality and without disturbing other equipment in the vicinity.

Electromagnetic interference can have various effects: a slight disturbance of the TV image, an error during a data transfer or even the complete and irreversible destruction of an electronic device.

The electrical system is a network of connected electrical components for the purpose of supplying, transferring and using electricity. The ambient electromagnetic environment represents all the electromagnetic phenomena that exist in a certain space area. [32], [33]

Electromagnetic interference is defined as an electromagnetic disturbance that interrupts, degrades or limits the performance of electronic / electrical equipment. The result of an interference phenomenon is a disturbance. [34]

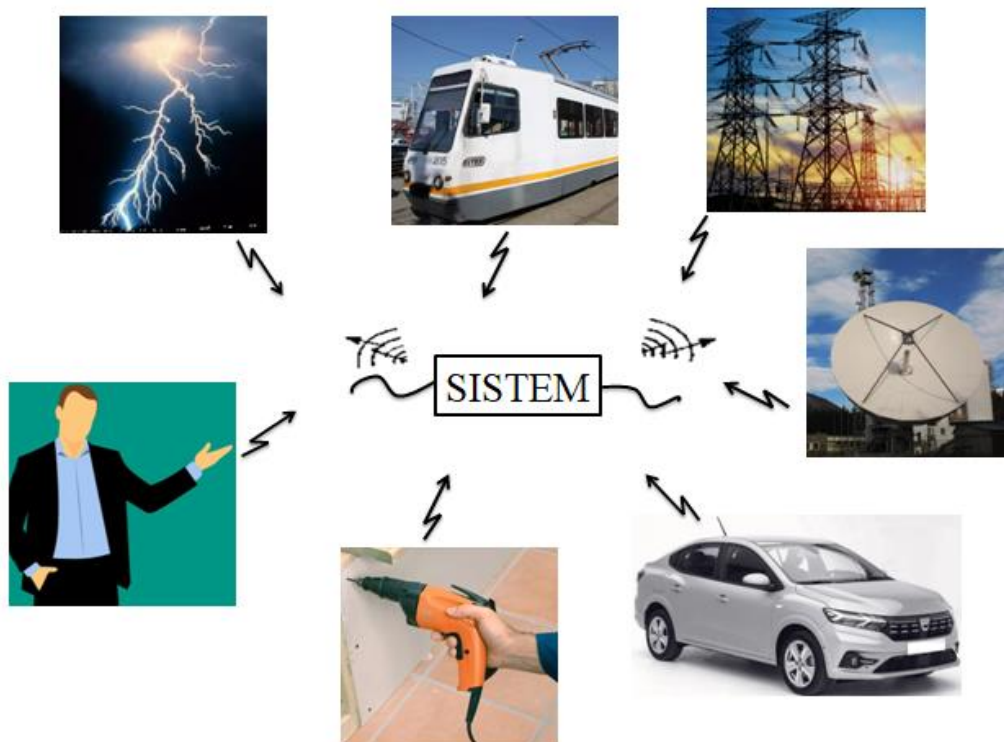


Figure 1.1. *Electrical system and surrounding space*

1.4. Brief history of electric vehicles

In 1801, Richard Trevithick built a steam carriage, opening the era of horseless mobility. After 30 years of noisy and dirty steam engines, the first battery-powered electric vehicle was built in 1834.

After 50 years, the first internal combustion engine was built in 1885.

In the 1910s, several hundred thousand electric vehicles were produced and used as personal vehicles, vans, taxis, and buses.

Charles Kettering's 1912 invention of the electric starter for internal combustion engines tipped the scales to cheaper internal combustion engines (1908 - Henry Ford produces the \$ 290 gasoline car, while a worker's annual salary was \$ 500).

In 1970, the return of electric vehicles began with energy problems caused by the oil crisis in the Middle East.

In the last part of the 20th century and the beginning of the 21st century, the electric vehicle began to regain ground in the automotive industry due to new regulations related to environmental protection and due to the development and improvement of rechargeable batteries, engine and controllers.^{[1], [4]}

1.5. Electromagnetic compatibility testing for electric vehicles

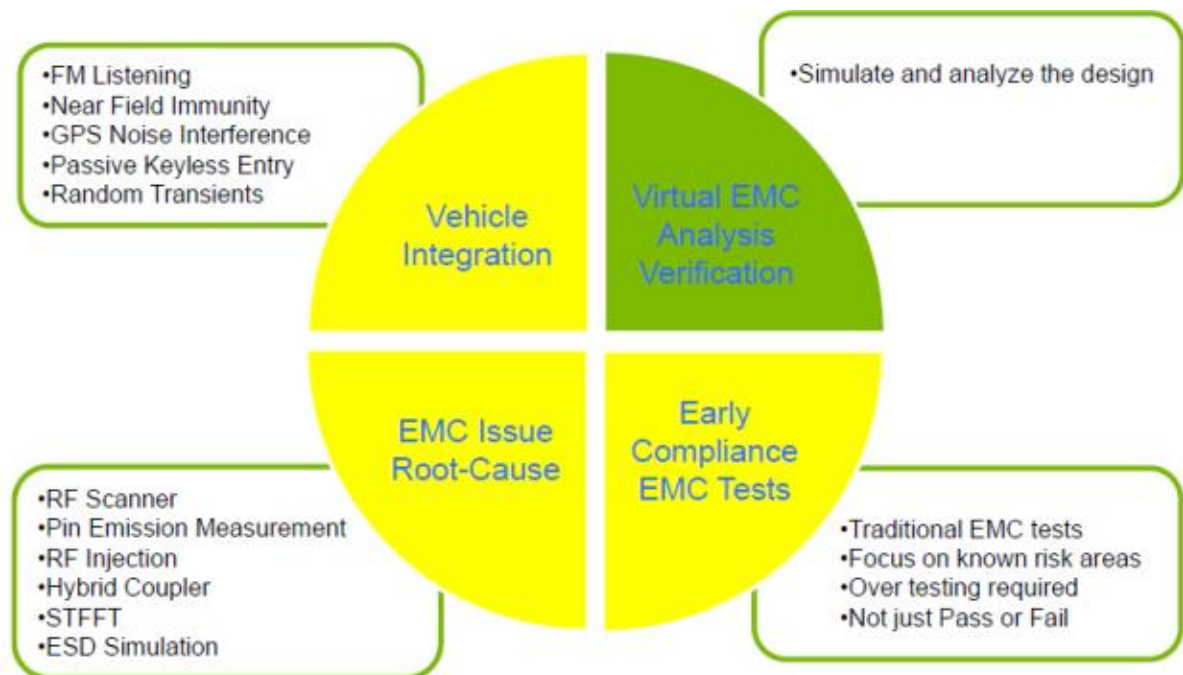


Figure 1.2: Pre-conformance testing process

Chapter 2: Structures of electric vehicles

All vehicles are devices that operate on the principle of energy conversion, transforming energy into mechanical torque that then reaches the wheels and spins them. In a conventional machine, energy is stored in chemical form by the fuel in the tank. Chemical reactions take place inside the tank between the hydrocarbon molecules in the fuel that burn together with the oxygen to release heat. Electric vehicles also use chemical energy stored in batteries, which they release electrochemically, without any combustion.

2.1. Vehicle with electric battery (BEV)

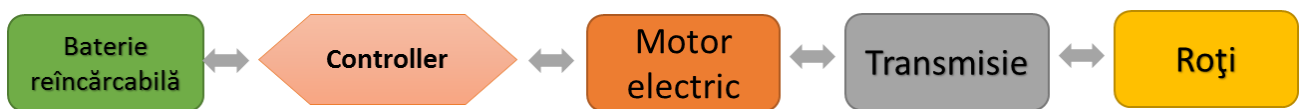


Figure 2.1: Energy flow for BEV

2.2. Hybrid electric vehicle (HEV)

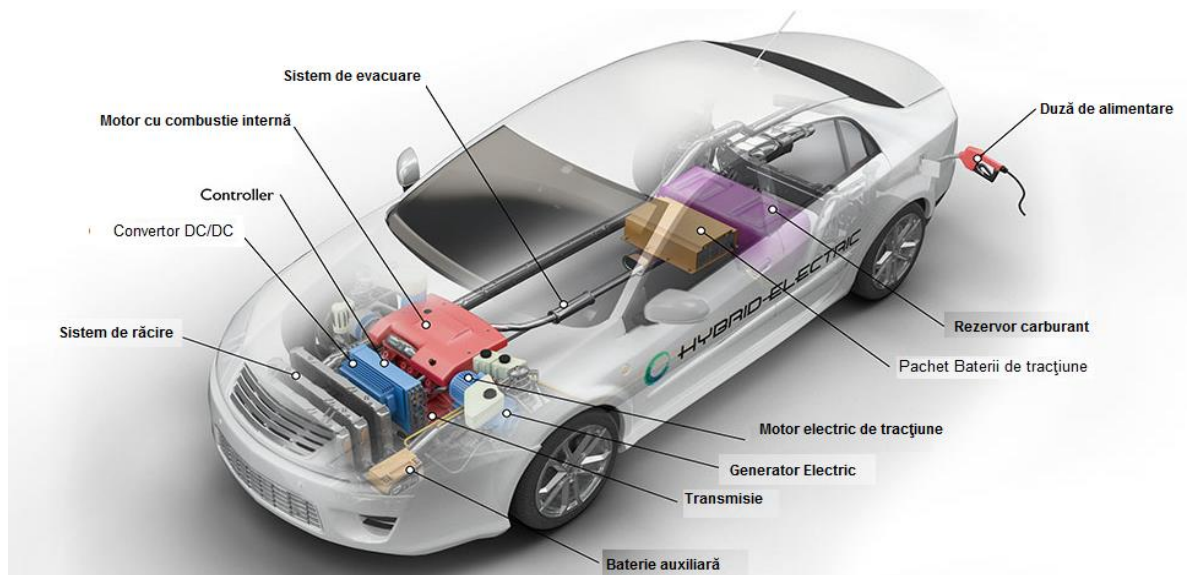


Figure 2.2: Hybrid Electric Vehicle (HEV) Components ^[5]

2.3. Hybrid plug-in vehicle (PHEV)

A. PHEV-series



Figure 2.3: Energy flow for PHEV-series

B. Parallel PHEV

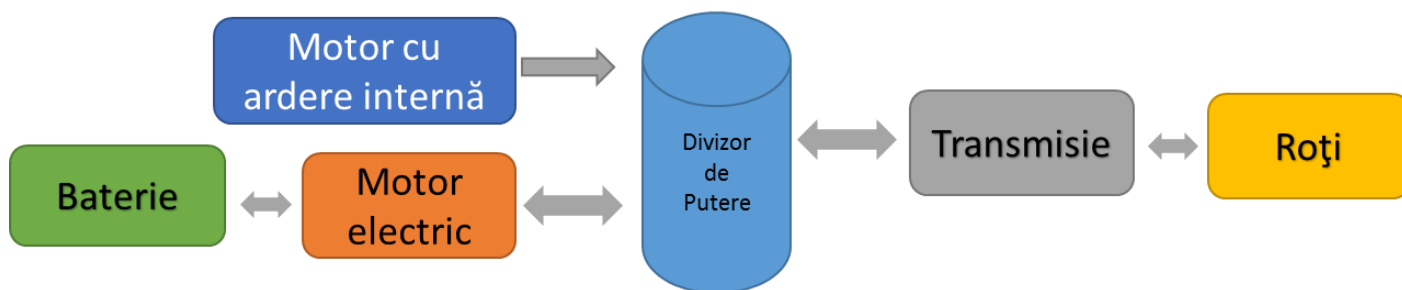


Figure 2.4: Energy flow for parallel PHEV

2.4. Integration of the electrical / electronic system in electric vehicles

In an electric vehicle, the internal high voltage network includes at least one energy storage unit and an electronic converter. The most popular variants of electric vehicles are composed of several interconnected electronic subsystems, which operate in direct current, at high voltages.

It is very important that the high voltage network of the vehicle is galvanically isolated from the low voltage network, but also from the chassis of the vehicle. The high voltage network must have insulated cables and connectors. ^[24]

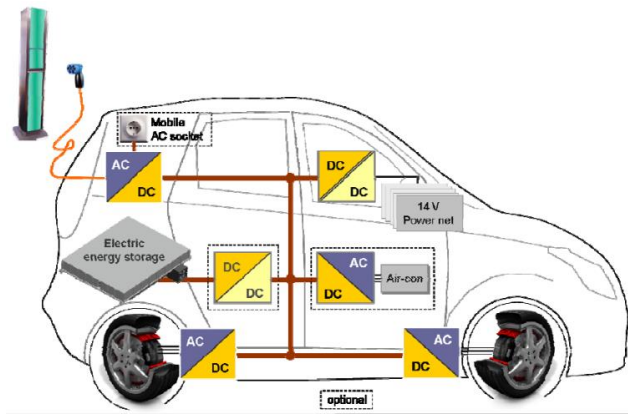


Figure 2.5: Basic structure of the high voltage network in an electric vehicle [24]

This simple construction solution has many advantages such as good cooling, accessibility in case of defect, but all this contrasts with the main disadvantage, that of the need for an expensive box, quite large and difficult to integrate into the existing engine compartment.

An alternative solution, which eliminates all the disadvantages mentioned above, is shown in Figure 2.6. [24]

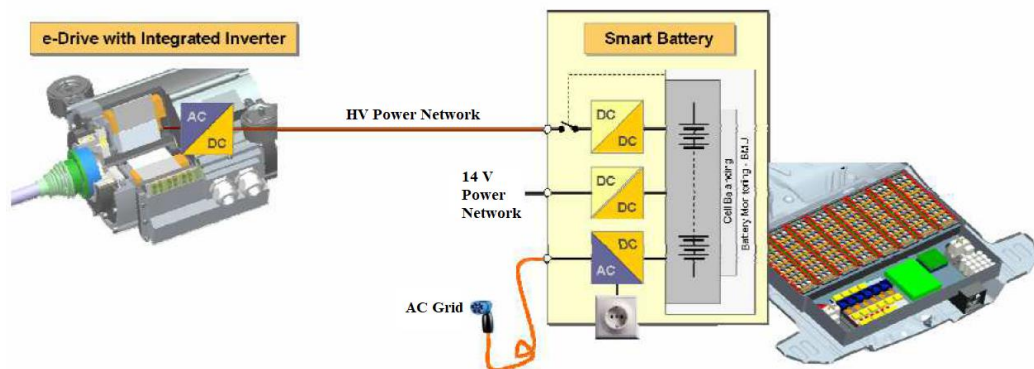


Figure 2.6: Integration of power electronics directly into the traction motor [24]

Chapter 3: Significant electromagnetic field sources in electric vehicles

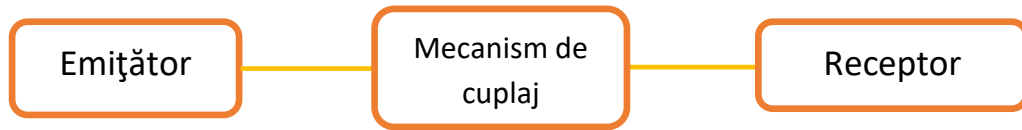


Figure 3.1: Interference pattern

3.1. Static converter

A few design aspects are essential for automotive applications: low weight, high efficiency, low volume, low electromagnetic interference.

3.2. Electric motor

The electric motor converts electrical energy into mechanical energy. They are capable of delivering high starting torque even at a speed of 0 km / h.

AC motors are lighter than DC motors. The controller design is more complex. The three-phase induction motor and the synchronous motor are the most used for the construction of electric vehicles.

3.3. Battery

Types of batteries used in the construction of electric vehicles

- Battery with Pb and sulfuric acid
- Nickel metal hydride battery
- Lithium-Ion Battery ^[8]

3.4. Shielded and unshielded cables

The cables of the high voltage bus, connecting the power converter to the motor and the power source, must be considered for the description of the new electric vehicle drive system.

In terms of electromagnetic compatibility, there are high voltage lines that carry voltages up to 900 V. ^[8]

3.5. Coupling mechanisms

The electric vehicle drive system contains several components that are only connected to the new high voltage bus. The level of electromagnetic interfaces between the conventional electrical system and low voltage devices such as the radio receiver must be protected in the integration of the new components of the drive system.

In addition to the interconnection of the lines, another coupling mechanism is the electromagnetic interference radiated by the high voltage cables inside the vehicle.^[8]

The interference is an unintentional transfer of electromagnetic energy. The effect of the interference phenomenon is disturbance.

The interference from the source to the receiver is transmitted through one of the following coupling mechanisms:^[33]

3.5.1. Galvanic coupling (conductive)

Conductive coupling occurs when the coupling path between the source and receiver is formed by direct electrical contact with a conductive body.^[33]

3.5.2. Magnetic coupling (inductive)

Inductive coupling refers to the phenomenon that exists when a magnetic field produced by an electric current in one circuit induces an effect on a magnetic flux produced by another circuit. When this happens, the two fluxes become reactive with each other or coupled by the inductive effects of time-varying magnetic fields.

3.5.3. Electrical coupling (capacitive)

The coupling is due to the existence of parasitic capacitances. This type of coupling occurs between conductors that have different electrical potentials. This type of coupling may have an intentional or accidental effect.

3.5.4. Electromagnetic radiation coupling

Electromagnetic radiation coupling occurs when the electromagnetic energy emitted by a source propagates and induces voltages and currents in another circuit near or far, the electromagnetic field propagating at the speed of light.^[33]

Chapter 4: Electromagnetic compatibility Standards

Magnetic field exposure measurement is a two-step process: first, it must characterize the magnetic field inside the vehicle (either by estimation or by measurement). The second step involves determining whether the values obtained may be harmful to passengers or not. There are certain standards in this regard that help us determine the second step.

4.1. ICNIRP regulations

Frecvența (Hz)	Intensitatea câmpului magnetic H (A/m)	Inducția magnetică B (T)
1-8 Hz	$3.2 \times 10^4/f^2$	$4 \times 10^{-2}/f^2$
8-25 Hz	$4 \times 10^3/f$	$5 \times 10^{-3}/f$
25-400 Hz	1.6×10^2	2×10^{-4}
400-3 kHz	$6.4 \times 10^4/f$	$8 \times 10^{-2}/f$
3 kHz-10 MHz	21	2.7×10^{-5}

Tabel 4.1: ICNIRP reference levels for public exposure to time-varying magnetic fields.^[9]

4.2. Static magnetic field exposure regulations

In table 4.2 are presented the limits to static magnetic field for occupational exposure which can be applied to those people which may be exposed everyday to static magnetic field because of their profession and also for general public which is referring to the entire population:

Exposure Characteristics	Magnetic field flux density (B)
<i>Occupational</i>	
Exposure of head and trunk	2T
Exposure of limbs	8T
General public	
Exposure to any part of the body	400 mT

Tabel 4.2. LIMITS OF EXPOSURE TO STATIC MAGNETIC FIELD ^[27]

4.3. IEEE Exposure Standard

Frecvența (Hz)	Intensitatea câmpului magnetic H (A/m)	Inducția magnetică B (T)
< 0.153 Hz	9.39×10^4	118×10^{-3}
0.153-20 Hz	$1.44 \times 10^4/f$	$18.1 \times 10^{-3}/f$
20-759 Hz	719	0.904×10^{-3}
759-3 kHz	$5.47 \times 10^5/f$	$687 \times 10^{-3}/f$

Table 4.3: IEEE - Maximum permitted level of exposure to the sinusoidal magnetic field for the general public: head and chest.^[9]

4.4. Electromagnetic compatibility Standards in Automotive

TABLE 4.4: AUTOMOTIVE CONDUCTED IMMUNITY REQUIREMENTS ^{[18], [20]}

Doc. Nr.	Title	Equivalent	Test Setup
SAE J113/11	Immunity to conducted transients on power leads	ISO 7637-2	Immunity to conducted transients
SAE J113/12	Electrical Interference: Conduction and Coupling - Capacitive and Inductive Coupling via Lines, other than Supply Lines	ISO 7637-3	Immunity to conducted disturbances generated by different coupling mechanisms
ISO 11452 - 10	Methods of component testing for electrical disturbances from narrowband radiated electromagnetic energy - Part 10: Immunity to conducted disturbances in the extended audio frequency range	SAE J1113/2	Immunity test on conducted radioations between 15 Hz – 500 MHz
ISO 7637-2	Road vehicles - Electrical disturbances produced by conduction and coupling - Part 2: Electrical transient conduction along supply lines only	SAE J113/11	Conducted electrical transients along supply lines only
ISO 7637-3	Vehicles with nominal supply voltage: 12 V or 24V - Electrical transient transmission by capacitive and inductive coupling via lines other than supply lines	SAE J113/12	Conducted immunity to different coupling mechanisms

TABLE 4.5: AUTOMOTIVE RADIATED IMMUNITY REQUIREMENTS [18], [20]

Doc. Nr.	Title	Equivalent	Test Setup
SAE J551/16	Reverberation Chamber Method: EMI (Electromagnetic immunity) - Off-Vehicle Source - Part 16 - Immunity to Radiated Electromagnetic Fields	-	It is needed a reverberation chamber, dimensioned for vehicles
SAE J551/17	Vehicle EMI - Power Line Magnetic Fields	-	Immunity test to magnetic field radiations
SAE J113/4	Bulk current injection (BCI) method Immunity to radiated electromagnetic fields	ISO 11452-4	Radiated immunity using the BCI method
SAE J113/27	EMC Measurements Procedure for Vehicle Components - Part 27: Immunity to Radiated Electromagnetic Fields - Reverberation Method	-	Reverberation chamber specifications based on SAE J113/27-1995 (or General Motors Engineering Standards)
ISO 11451-2	Vehicle test methods for electrical disturbances from narrowband radiated electromagnetic energy – Part 2: Off Vehicle Radiation Sources	SAE J551-11	Vehicle Radiated Immunity test in a anechoic chamber
ISO 11451-3	Simulation of on-board transmitter	SAE J551-12	Vehicle Absorber Lined Shielded Enclosure
ISO 11451-4	BCI	SAE J551/13	Test designed for machines and vehicles too big to fit in a standard vehicle EMC
ISO 11452-2	Component test methods for electrical disturbances from narrowband radiated electromagnetic energy – Part2: Absorber lined chamber	SAE J1113/2 1	There are needed an absorber lined chamber, antennas and field generators to cover the range. Not necessary to scan.
ISO 11452-3	Transverse electromagnetic (TEM) cell	SAE J1113/2 4	TEM cell
ISO 11452-4	BCI	SAE J1113/4	Radiated immunity - BCI
ISO 11452-5	Stripline	SAE J1113/2 3	Radiated immunity using a stripline
ISO 11452-7	Direct radio frequency (RF) power injection	SAE J1113/3	Conducted immunity test 250 kHz to 500 MHz
ISO 11452-8	Magnetic field immunity	SAE J1113/2 2	Are used Helmholtz coils

ISO 11452-9	Portable transmitters	-	Small antennas are used together with amplifiers and signal sources to simulate portable transmitters
ISO 11452-10	Immunity to conducted disturbances - extended audio frequency range	SAE J1113/2	Conducted immunity test in range of 15 Hz to 500 MHz
ISO 11452-11	Reverberation Chamber	SAE J1113/2 8	Reverberation chamber – Mode Tuned

TABLE 4.6: AUTOMOTIVE RADIATED EMISSIONS REQUIREMENTS ^{[18], [20]}

Doc. Nr.	Title	Equivalent	Test Setup
SAE J551/5	Magnetic and electric field strength measurement methods and performance levels for EVs. Range: 150 kHz to 30 MHz	It is developing CISPR36 which will cover RE<30 mHz	Vehicle Absorber Line Chamber is necessary
CISPR12	Characteristics of radio disturbance for boats, vehicle and internal combustion engines — Methods and limits' measurement for off-board receivers protection	SAE J551/2	Radiated Emissions
CISPR25	Characteristics of radio disturbances for boats, vehicle and internal combustion engines – Methods and limits' measurement for on-board receivers protection	SAE J551/4	Clause 5: Dedicated part of the standard for vehicles. Measurement of the noise amount produced by the vehicle induced into the on-board receiver antenna port.
CISPR25	Characteristics of radio disturbances for boats, vehicle and internal combustion engines – Methods and limits' measurement for on-board receivers protection	SAE J1113/4 1	Clause 6: Measurement of conducted and radiated emissions for component test section.

TABLE 4.7: AUTOMOTIVE ELECTROSTATIC DISCHARGE REQUIREMENTS ^{[18][20]}

Doc. Nr.	Title	Equivalent	Test Setup
SAE J551 /15	Vehicle Electromagnetic Immunity Test –ESD	ISO-10605 Clause 10	Vehicle level ESD test without need of a shielded enclosure.
SAE J1113 /13	Vehicle components level - Electromagnetic compatibility procedure - immunity to ESD	ISO-10605	ESD testing procedure performed on bench at a controlled temperature and humidity environment
ISO - 10605	Road vehicles – Methods for testing electrical disturbances from ESD	SAE J551 /15 SAE J1113 /13	ESD testing performed on a module (bench or a vehicle) at a controlled temperature and humidity environment



4.5. UNECE Regulation 10

From the point of view of regulations R10.05 there are two categories of tests for electromagnetic interference radiation: broadband emissions (broadband → BB) caused by ignition systems, DC motors and on-board charging systems and narrowband emissions (narrowband → NB) produced by power converters, clock signal harmonics or anything other than arc or ignition. The limits are defined both for the vehicle as a whole and for component testing. ^[17]

4.6. CISPR Standard 25

4.6.1. Antenna systems for CISPR 25

Table 6.5 shows some of the electric field antennas used by CISPR25 and the frequency range in which they operate.

Antenna type		Frequency range	
Electrică	Biconică	30 MHz – 300 MHz	
	Log-periodică	200 MHz – 1 GHz	


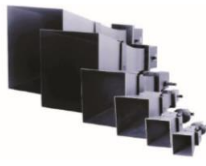

	Hibridă (BiLog, BiConiLog)	30 MHz – 1 GHz	
	Horn	1 GHz – 2.5 GHz	
Magnetică	Buclă, Cadru	9 kHz – 30 MHz	

Table 6.5: Broadband antennas for EMC tests ^{[16] [17]}

4.6.2. Anechoic Room

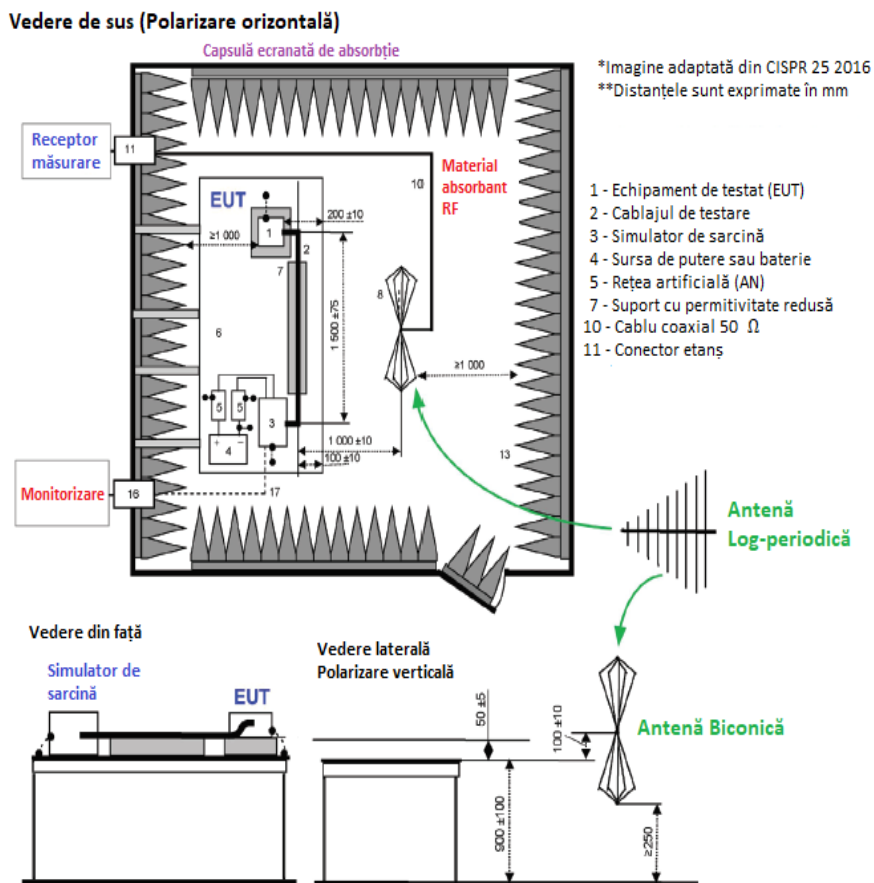


Figure 6.1: CISPR 25 Structure of measuring radiated emissions with biconical antenna (30 MHz - 300 MHz) or with log-period antenna (200 MHz - 1 GHz) ^[17]

4.7. ISO 11452 Standard



Figure 6.2: ISO 11452 test methods: TEM cell, stripline method, BCI method ^[19]

4.8. Possible victims of electromagnetic interference

In the case of electric vehicles, passengers sit very close to electrical systems that have significant power, usually for considerable periods of time. The drive system of electric vehicles is an electrical system with a considerable electrical power ranging from 40 to 120 kW. These power levels are mostly achieved by high currents rather than high voltages. Most commercial electric vehicles work with voltages around 400 V, which involve currents of hundreds of amperes. This means that the traction system can generate a strong magnetic field compared to other conventional sources.

Another effect that appears is called electromagnetic radiation and belongs to the field known as bioelectromagnetism, which studies the interaction between electromagnetic fields and biological systems. Electromagnetic radiation is mainly divided into ionizing and non-ionizing radiation, depending on the ability to ionize atoms and break chemical bonds. The boundary between ionizing and non-ionizing radiation is located in the ultraviolet range of the electromagnetic spectrum. In this sense, all electromagnetic radiation emitted by an electric vehicle is non-ionizing. [9]

Rapid charging of batteries is another situation where passengers or even pedestrians can be exposed in the vicinity of the vehicle. As battery technology has developed, higher charging rates are achieved, which implies higher currents, therefore stronger magnetic fields. As a general rule, during fast charging it is recommended that passengers sit outside the vehicle, at some distance from it.

Chapter 5: Simulation of the magnetic field inside the electric vehicle

5.1. Simulation environment

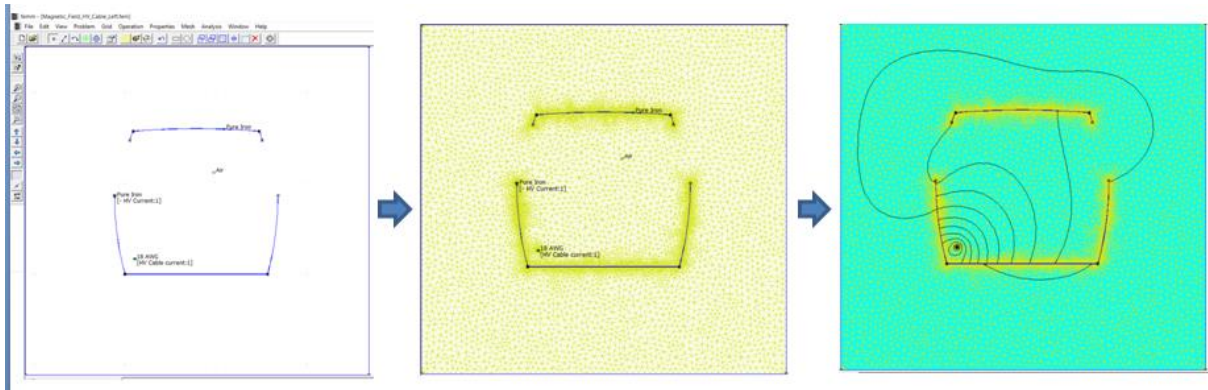


Figure 5.1: The three parts of the FEMM program

Figure 5.1 describes the three parts of the FEMM program applied to the chosen geometry. The image on the left shows the chosen geometry, the materials used, the circuit elements and the properties of the magnetic problem. The figure in the middle shows the chosen pattern divided into a large number of triangles. The representation can be seen in the figure on the right.

5.2. Geometry chosen for magnetic field simulation

A front view of the electric vehicle will be used to simulate the magnetic field produced by the high voltage cable that connects the electric motor to the battery system. As reference dimensions, the BMW i3 was taken as an example for simulation geometry which can be seen in Figure 5.2.

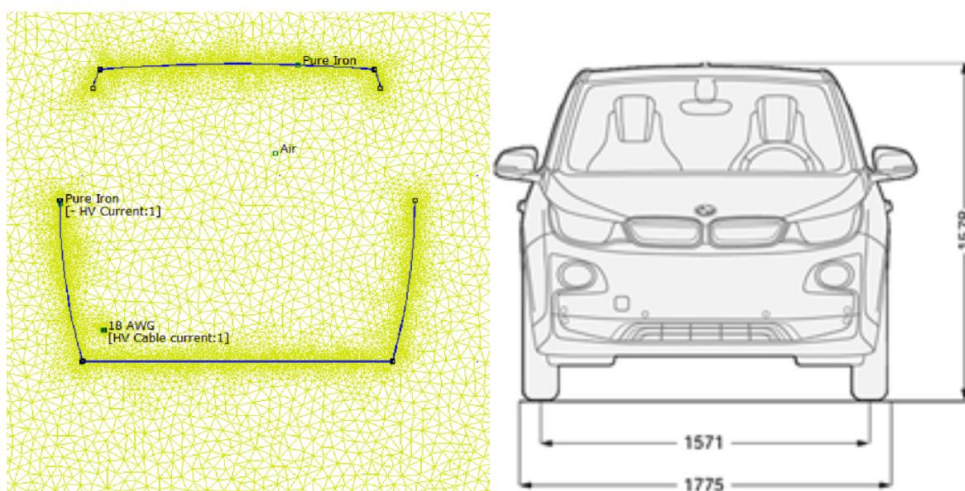


Figure 5.2: Simulation geometry - model geometry ^[30]

5.3. Cable track with return through the housing - asymmetrical construction

Figure 5.3 shows how the magnetic field lines are concentrated around the high voltage cable, closing through the body. If we study the legend we can see that the values of magnetic induction can reach up to 0.1997 T in this configuration, a value that is reached inside the body car.

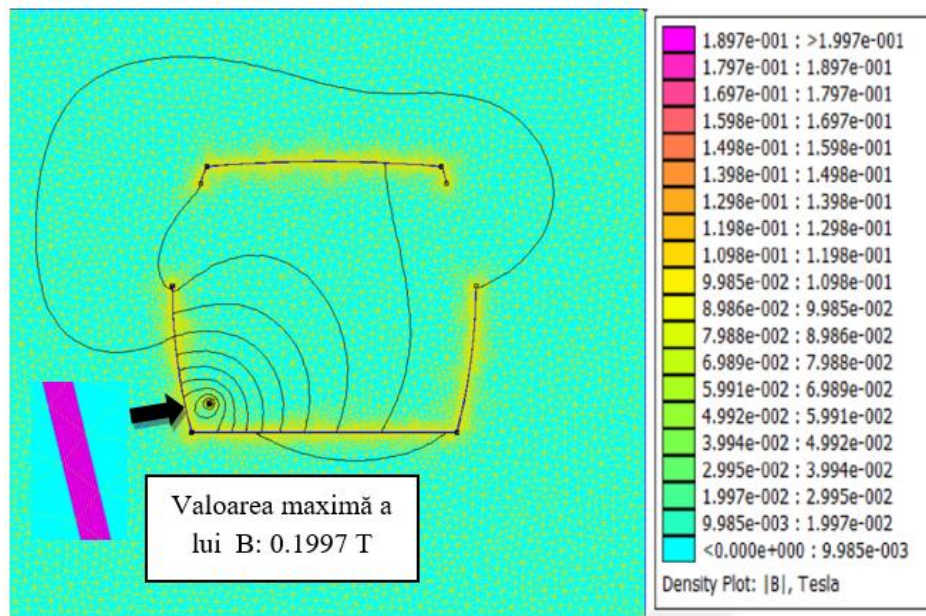


Figure 5.3: Representation of the magnetic field - asymmetric construction ^[30]

5.4. Round trip cable route - Symmetrical construction

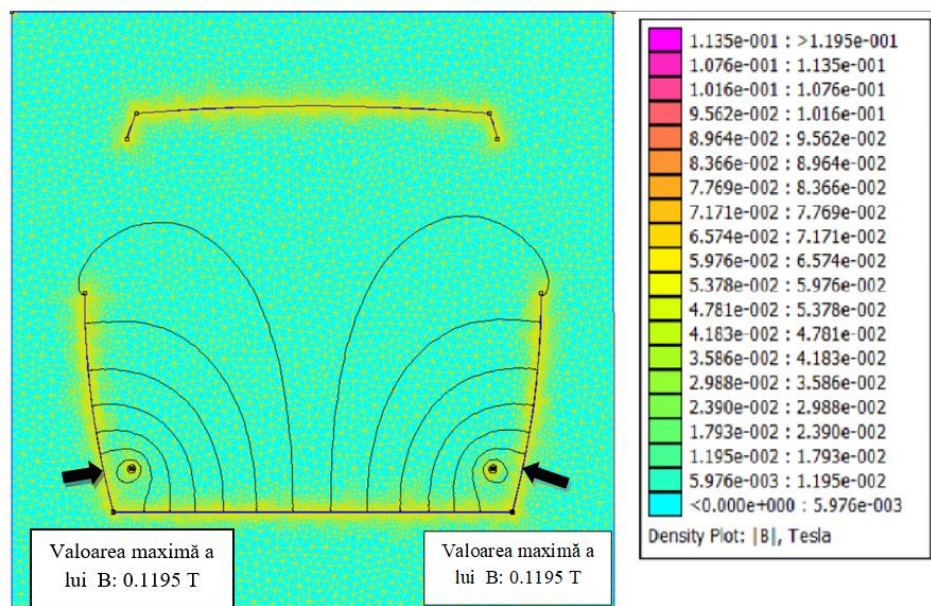


Figure 5.4: Magnetic field for symmetrical construction - Round cable

In Figure 5.4 you can see how the magnetic field lines are concentrated around the cables and close through the machine housing. Magnetic field values take values up to 0.1195 [T].

Comparing the case of symmetrical construction (back and forth cable) with the asymmetric one we can see that in the case of symmetrical construction the maximum value reached in the car body takes values lower by 0.2 [mT].

5.5. Wire path with housing return - symmetrical construction

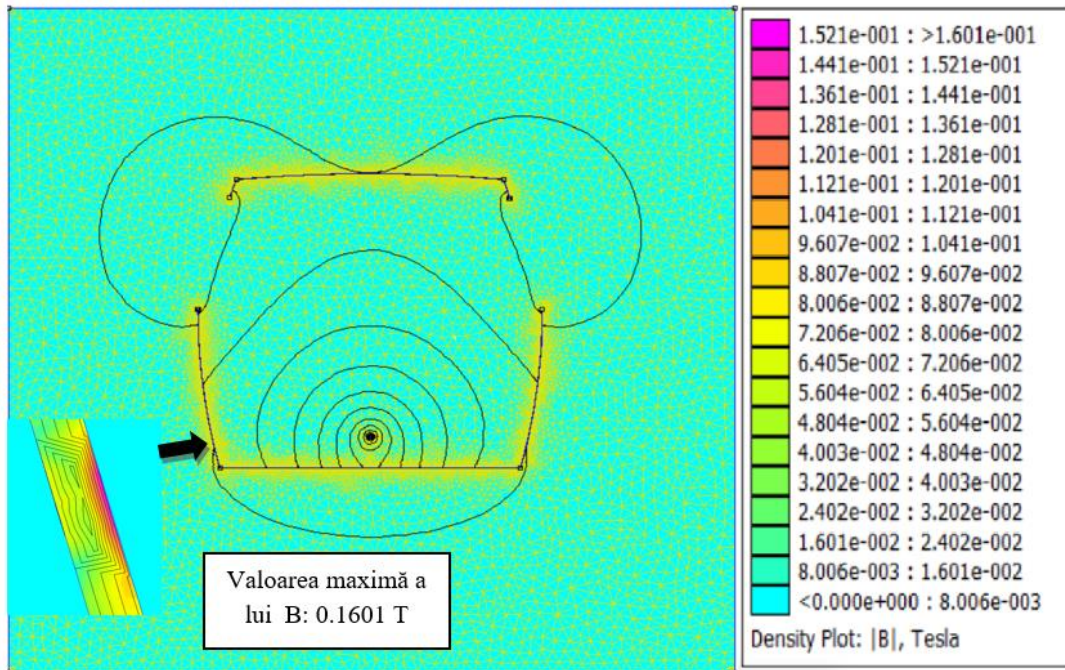


Figure 5.5: Representation of the magnetic field - symmetrical construction

Comparing with the first case the maximum values reached for the magnetic induction, we can observe that we obtain a lower magnetic induction by about 0.04 T.

5.6. Cable track with return by housing - symmetrical construction - 0 cm from the floor

In this case, the high voltage cable connecting the electric motor, which has the integrated inverter, to the intelligent battery system, will be positioned at 0 cm from the floor of the vehicle, symmetrically, in the middle of the car with return through the body.

Figure 5.6 shows the distribution of magnetic field lines near the cable and beyond. With this topology the values of the magnetic induction reach up to 0.295 T.

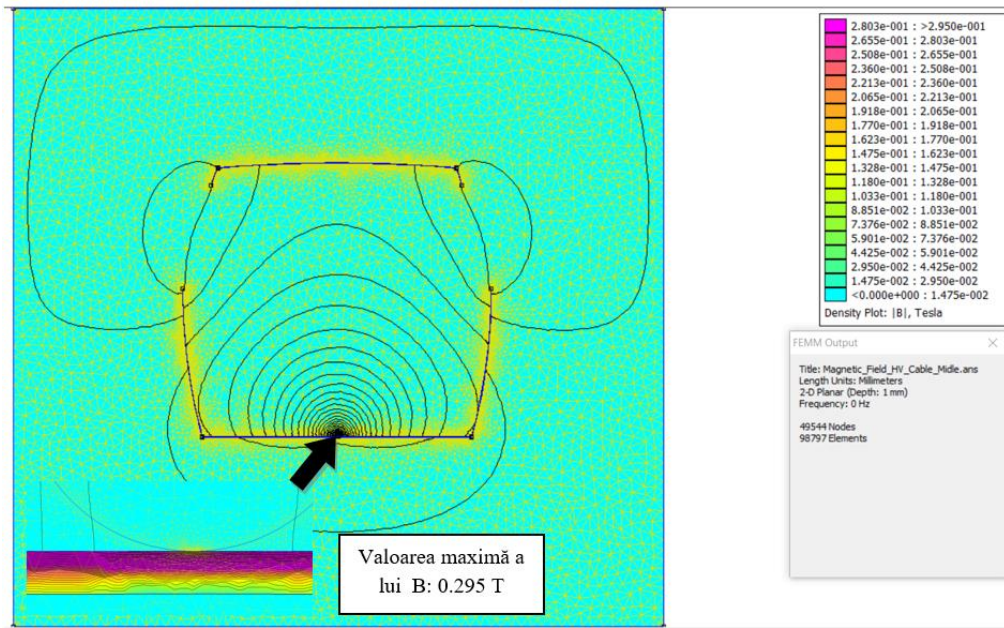


Figure 5.6: Representation of the magnetic field - symmetrical construction - 0 cm from the floor

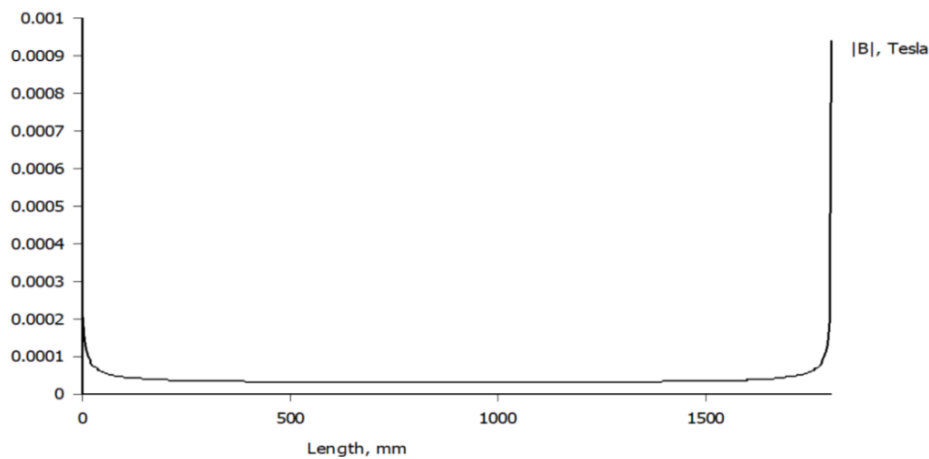


Figure 5.7: Graphical representation of the values of the magnetic field at the lower level of the windows inside the electric vehicle

5.7. Cable track with return by housing - symmetrical construction - 10 cm from the floor

The high voltage cable that connects the electric motor to the intelligent battery system will be positioned 10 cm from the floor of the vehicle with the car body lock. In this case, too, a 100 A positive circuit was assigned inside the copper cable, and a -100 A negative circuit was assigned inside the iron body.

Figure 5.8 shows how the magnetic field lines are concentrated around the high voltage cable, closing through the body. If we study the legend we can see that the values of magnetic induction can reach in this configuration up to 0.1883 T.

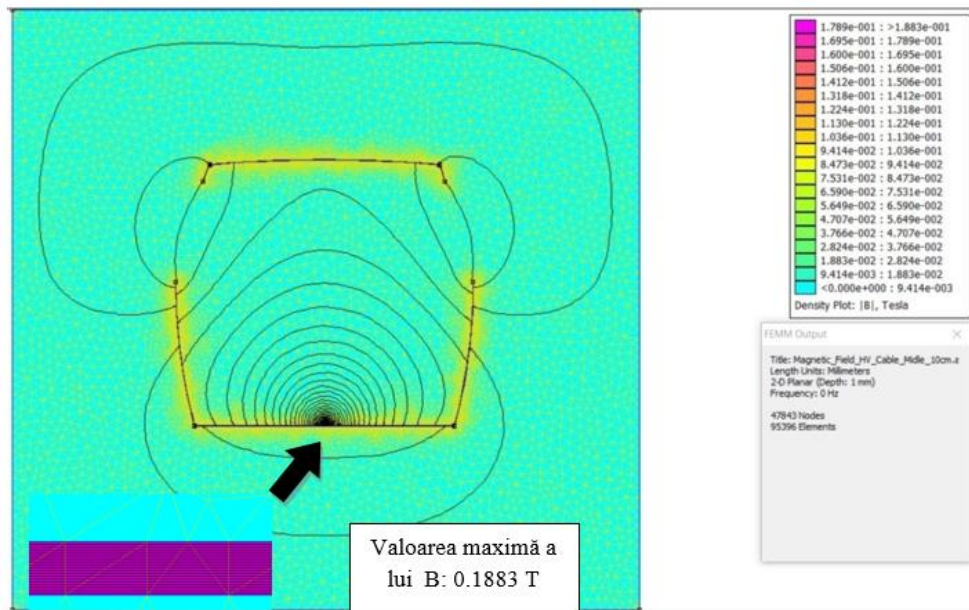


Figure 5.8: Representation of the magnetic field - symmetrical construction - 10 cm from the floor

Compared to the case study in which we have a symmetrical construction and the cable positioned at 0 cm from the floor, the maximum values reached for magnetic induction, we can see that we obtain a lower magnetic induction by about 0.1 T.

5.8. Cable track with return by housing - symmetrical construction - 10 cm from the floor with seats

In this case, the high-voltage cable that connects the electric motor to the intelligent battery system will be positioned 10 cm from the floor of the vehicle with the car body closure and the metal frame of the seats will also be represented. In this case, too, a 100 A positive circuit was assigned inside the copper cable, and a -100 A negative circuit was assigned inside the iron body.

Figure 5.9 shows how the magnetic field lines are concentrated around the high voltage cable, closing through the body and the metal frame of the seats. If we study the legend we can see that the values of magnetic induction can reach in the present configuration up to 0.2527 T.

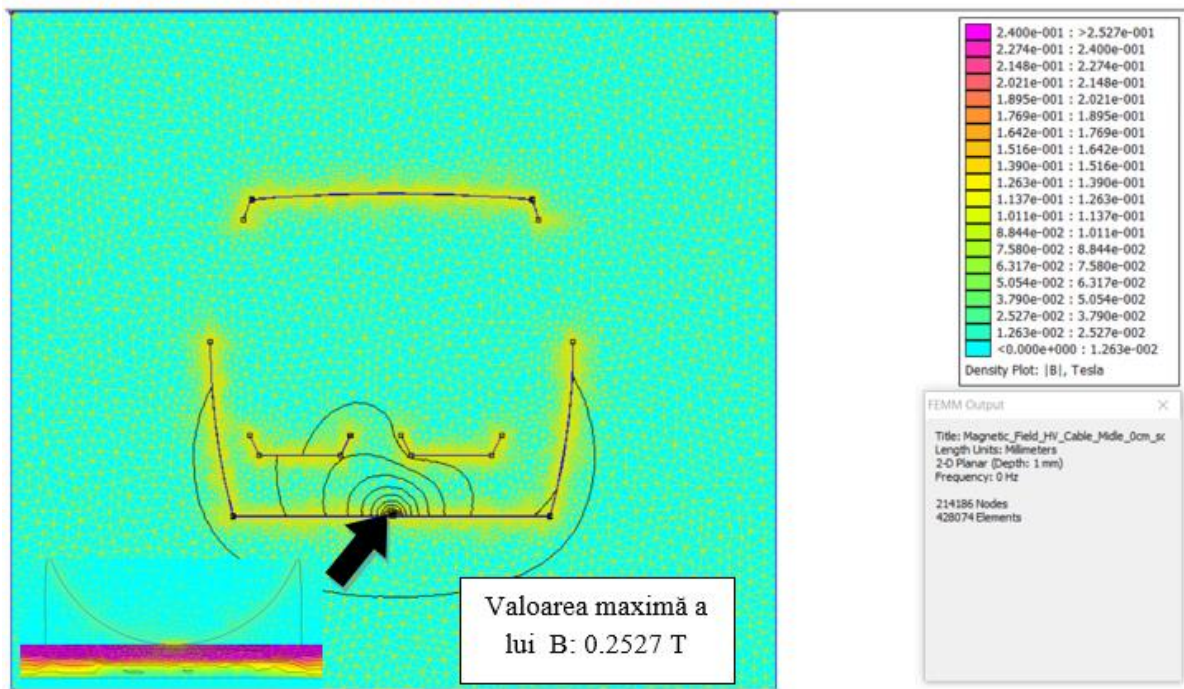


Figura 5.9: Reprezentarea câmpului magnetic – construcție asimetrică 10 cm față de podea cu scaune

Comparing with the other two cases in which we analyzed the symmetrical construction at 0 cm and 10 cm from the floor, respectively, the maximum values reached for magnetic induction, we can see that we obtain a magnetic induction lower by about 0.04 T compared to the case with 0 cm and higher by 0.06 T compared to the one positioned at 10 cm from the floor.

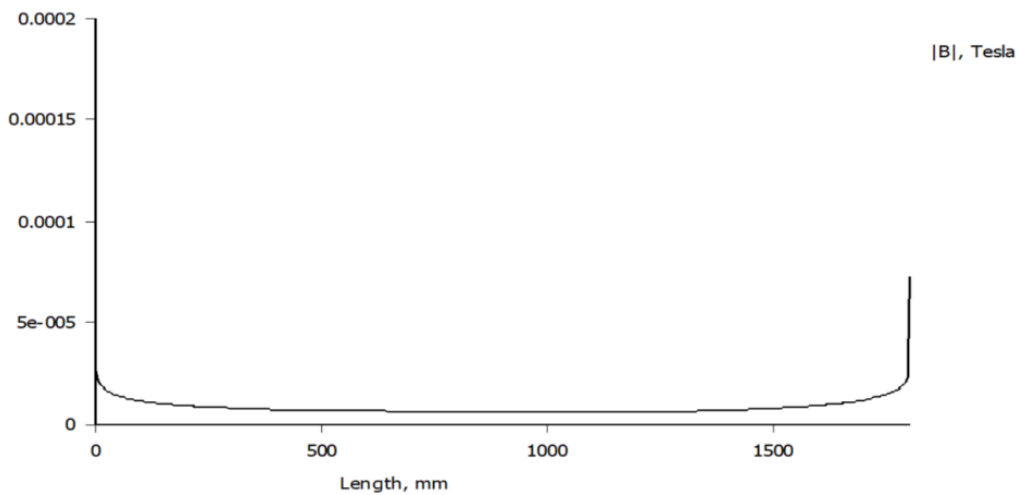


Figure 5.10: Graphical representation of the values of the magnetic field at the lower level of the windows inside the electric vehicle

5.9. Coaxial cable magnetic field simulation - asymmetric construction

Table 5.1 shows the dimensions of each layer of the coaxial cable and also the materials used. The simulated coaxial cable has a copper inner conductor, covered with silicone rubber insulation, insulated by a copper shield that is coated with another layer of silicone rubber.

	Conductor	Silicon rubber insulation	Copper shield	Silicon rubber insulation
Thickness [mm]	8.5	2	0.252	3.438

Table 5.1: Coaxial cable dimensions and materials

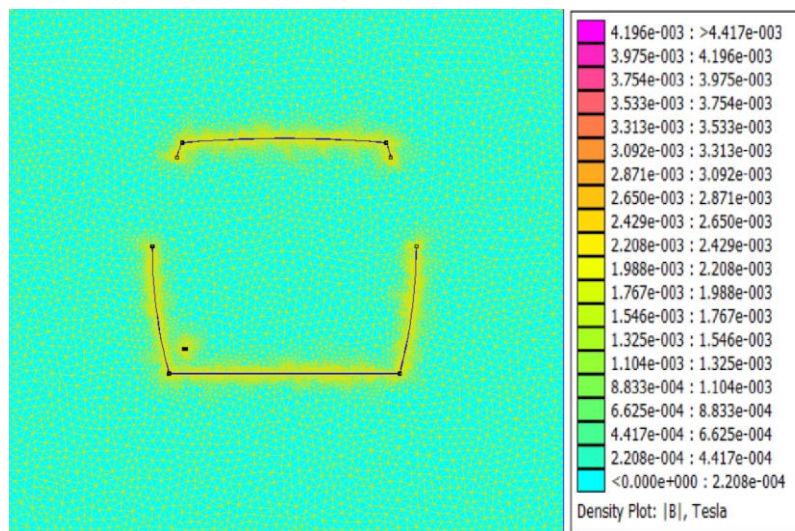


Figure 5.11: Representation of the magnetic field - coaxial cable in asymmetric construction ^[30]

It can be seen that in the case of coaxial cable for asymmetric construction, the magnetic flux lines close inside the cable, reaching maximum values of 4,417 mT.

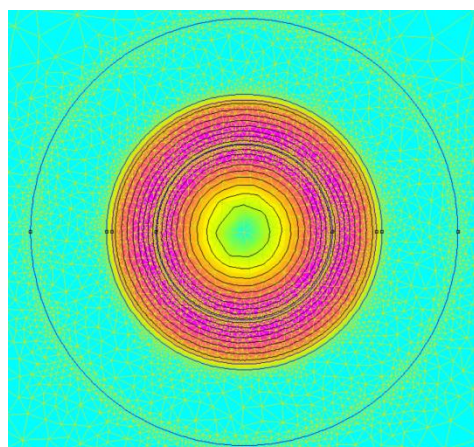


Figure 5.12: Representation of the magnetic field inside the coaxial cable ^[30]

Chapter 6: Study of the interaction between the surrounding electromagnetic environment and the electric vehicle

6.1. Description of the ambient electromagnetic environment

The electromagnetic spectrum covers electromagnetic waves with frequencies between 1 [Hz] and 1025 [Hz]. Figure 6.1 shows the distribution of electromagnetic fields from radio to gamma rays. [28]

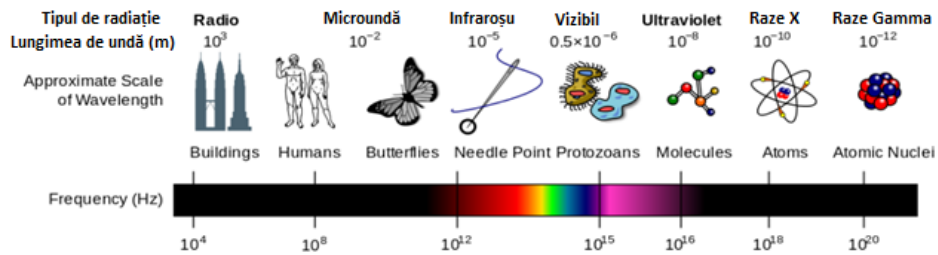


Figure 6.1: Electromagnetic spectrum [29]

6.2. Analysis and simulation of the electromagnetic environment outside the electric vehicle

Using the FEMM program, the simulation of the magnetic field produced by a 20 [kV] power distribution line was performed. The 3 active conductors of a pole represented in 2D were positioned at a height of 7m from the ground. The diameter of the conductors was chosen to be 20 mm, and the current flowing through the cables has the values $I_1 = 310\sqrt{3}$ [A], $I_2 = -310/2$ [A], $I_3 = -310/2$ [A]. The simulation was performed at 50 Hz, having alternative current.

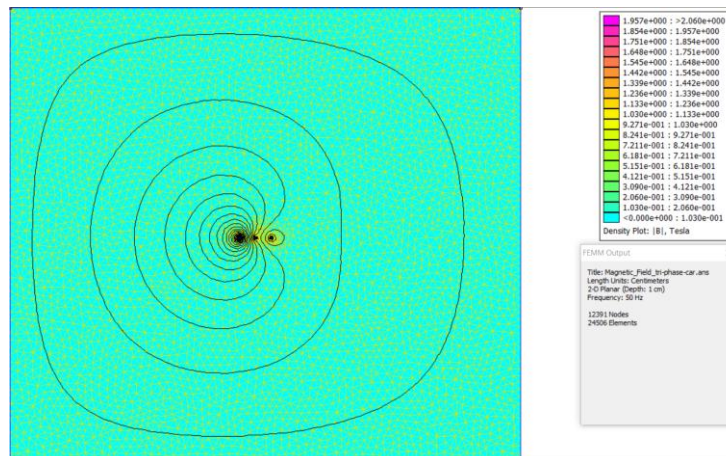


Figure 6.2: Magnetic field distribution of a three-phase MT distribution line [31]

It can be seen from Figure 6.2 how the magnetic field lines are distributed around the three-phase supply line. On the right is the legend that shows that the maximum value reached in this case is 2.06 [T]. Figure 6.3 shows the distribution of the magnetic field inside one of the 3 conductors. The maximum value of 2.06 [T] is reached on the cable contour.

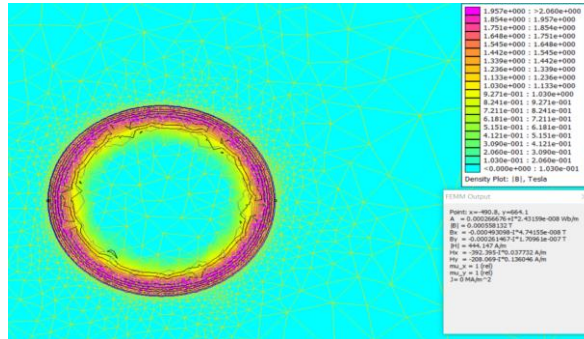


Figure 6.3: Distribution of the magnetic field inside a conductor of the power line [31]

6.3. Simulation of the magnetic field produced by a medium voltage power transfer line in the presence of a body car

In this case, a vehicle body was inserted. For the time being, no current circuit has been assigned to the housing, the purpose being to see how the electromagnetic medium interacts with the vehicle structure. Figure 6.4 shows the interaction of magnetic fields between the MT power transfer line and a vehicle cab. It can be seen that the density lines of the magnetic flux do not intersect with the car body.

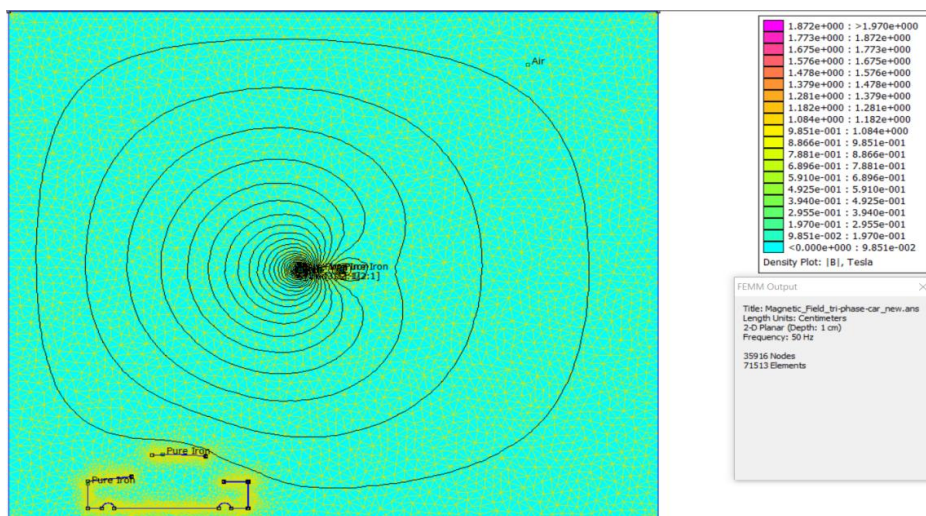


Figure 6.4: The interaction of the magnetic field between the electrical network and a body [31]

In Figure 6.5 you can see how the density lines of the magnetic field flux are distributed near the cable contour. The maximum value of 1.97 [T] is reached inside the conductor on its contour.

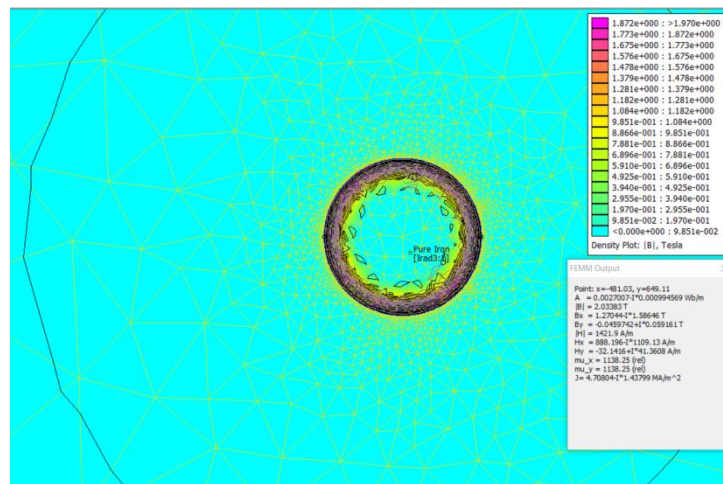


Figure 6.5: Distribution of the magnetic field inside a conductor of the power line in the presence of the EV cab [31]

6.4. Analysis of the ambient electromagnetic environment inside the passenger compartment of the electric vehicle

Electric vehicles mainly have 3 main sources of radiation from the magnetic field: - the intelligent battery system which includes the power converters used for charging the battery, connecting to the mains and managing voltage levels;

- the electric motor that can have the inverter integrated directly in it;
- the high voltage network of the machine that interconnects the intelligent battery system with the electric motor.

For this case, an electric vehicle body was introduced in the simulation in which a high voltage cable with a diameter of 8 [mm] and a current value of 100 [A] was inserted.

It will be analyzed how the magnetic field produced by the medium voltage supply network interacts with the high voltage network placed in the machine. To simulate the power of the cable inside the car, a 100 [A] circuit was assigned inside the Copper cable and another circuit of -100 [A] was assigned to the car body.

Figure 6.6 shows how the magnetic flux lines are distributed. In the legend we can see that the maximum value for the magnetic field flux density has values up to 2,061 [T], a value obtained inside the conductors of the supply line.

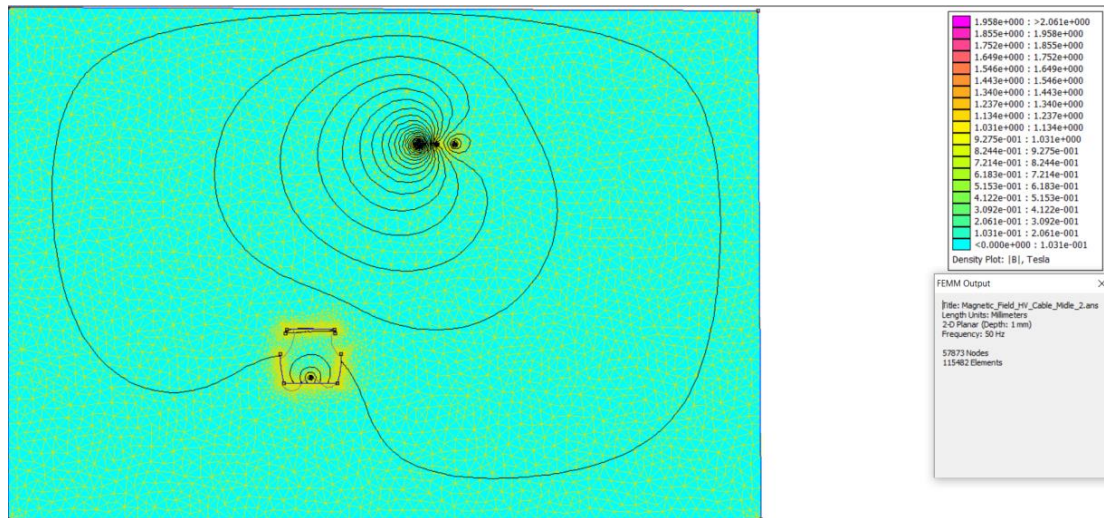


Figure 6.6: Interaction between the magnetic fields of the power supply and the HV network of the electric vehicle in symmetrical construction [31]

6.5. Electric and magnetic field measurement during charging of an electric vehicle

In the first case, the measurement sets highlight the magnetic and electric field values for the slow charging mode, using a Type 2 charger, in the frequency range 0 – 100 [Hz]. The charging power is 3.6 [kW] alternating current. It takes 11 hours 45 minutes to fully charge the battery.

In the second case, we studied the electric and magnetic field values for the fast charging mode, using a Chademo type charger, in the frequency range 0 – 100 [Hz]. The maximum charging power is 46 [kW] in direct current. It takes 40 minutes to fully charge the battery.

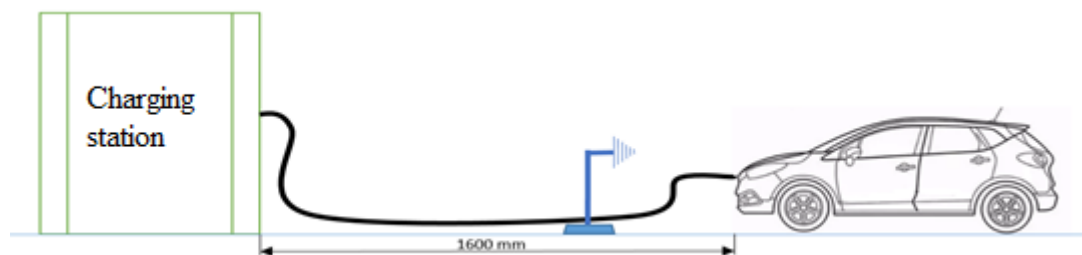


Figure 6.7: Vehicle diagram in charging mode connected to the electrical supply network

6.5.1. Electric and magnetic field measurement for slow charging

For this first set of electric and magnetic field measurements, we used a Type 2 charger connected directly to a 230 [V] conventional outlet. Measurements were made for 1 minute in the frequency range 0 - 100 [Hz] for slow AC charging.

In figure 6.8 I represented the values of electric field strength and magnetic induction, with the antenna positioned next to the car's charging connector.

From the represented graph we can see that the maximum value obtained for the electric field intensity is 111.15 [V/m], obtained at 50.05 [Hz]. The maximum value of the magnetic induction is also reached at the frequency of 50.05 [Hz] and is 0.0397 [μ T].

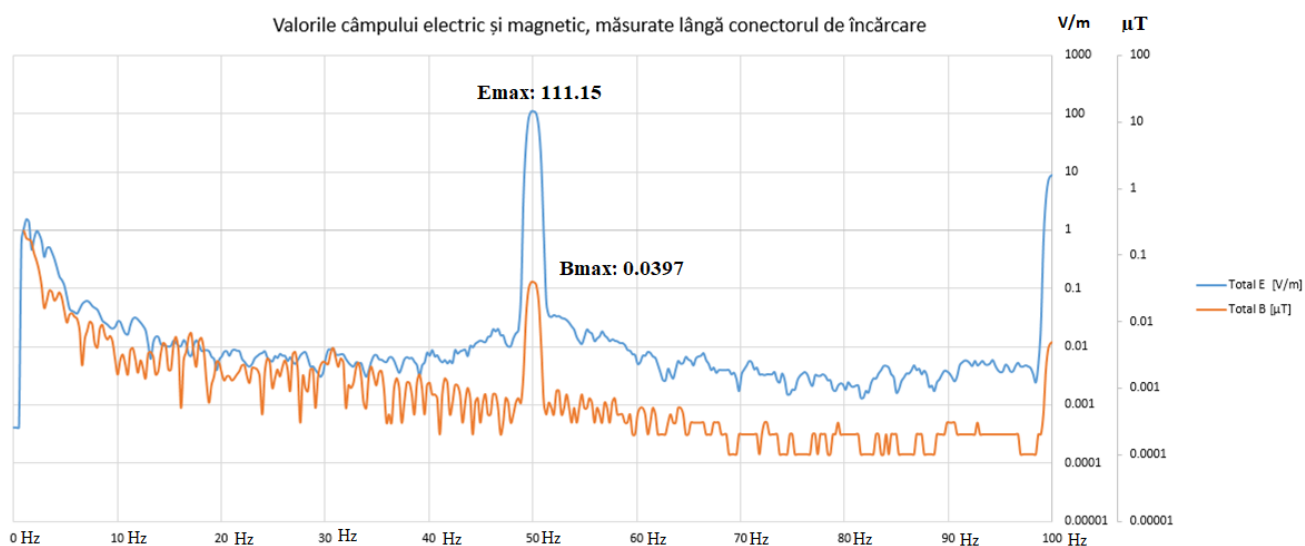


Figure 6.8: Representation of the magnetic and electric field in the frequency spectrum 0 – 100 Hz, for slow charging, antenna positioned near the charging connector

Comparing the values measured near the charging connector with the limits imposed by ICNIRP 2010 (see Table 4.1), we can see that the value of the magnetic field strength of 111.15 [V/m] is lower than the one imposed by the standard which is 5 [kV/m], as well as the magnetic induction of 0.0397 [μ T] is lower than the value imposed by the standard which is 2×10^{-4} [T].

In figure 6.9 we have represented the values of the electric field intensity and the magnetic induction, with the antenna positioned near the power socket.

From the represented graph we can see that the maximum value obtained for the electric field intensity is 185.03 [V/m], which is obtained at 50.05 [Hz]. The maximum value of the magnetic induction is also reached at the frequency of 50.05 [Hz] and is 0.8226 [μ T].

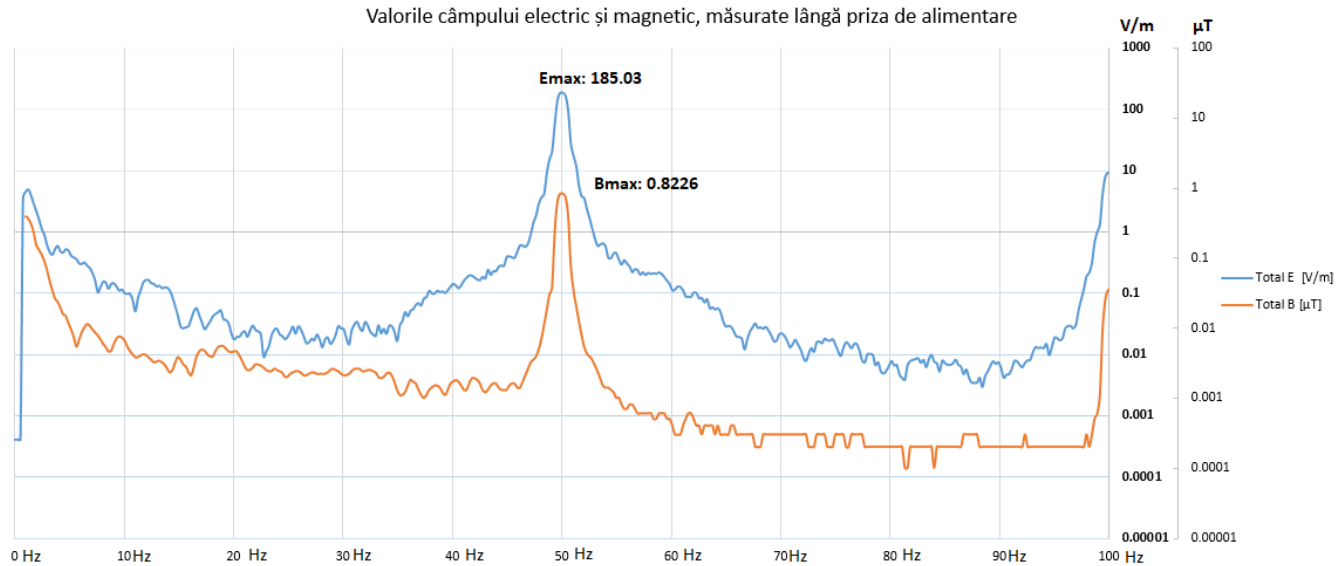


Figure 6.9: Representation of the magnetic and electric field in the frequency spectrum 0 – 100 Hz, for slow charging, the antenna positioned near the power outlet

Comparing the values measured near the power outlet with the limits imposed by ICNIRP 2010 (see Table 4.1), we can see that the value of the electric field intensity of 185.03 [V/m] is lower than the one imposed by the standard which is 5 [kV/m], as well as the magnetic induction value of 0.8226 [μ T] is lower than the one imposed by the standard which is 2×10^{-4} [T].

It is useful to compare the values obtained in the 2 topologies. For the electric field intensity we obtained 111.15 [V/m] near the power connector, a value that is lower than the one obtained for the measurement made near the power socket: 185.03 [V/m]. And in the case of magnetic induction we noticed that the value of 0.0397 [μ T] measured near the car's power connector is lower than 0.8226 [μ T] measured near the power outlet.

6.5.2. Electric and magnetic field measurement for fast charging

To ensure that the tests are not significantly affected by a false external noise or signal, an ambient noise measurement should be performed before the actual testing. This measurement was made on the left side, next to the car for a duration of 1 minute, in the frequency range 0 – 100 Hz. We are interested in the values measured around the frequency of 50 Hz. The maximum values obtained for E are 0.0268 [V/m] and for B are 0.0062 [μ T] as can be seen in Figure 6.10. These measured values for reference are acceptable and do not alter measurements taken during charging.

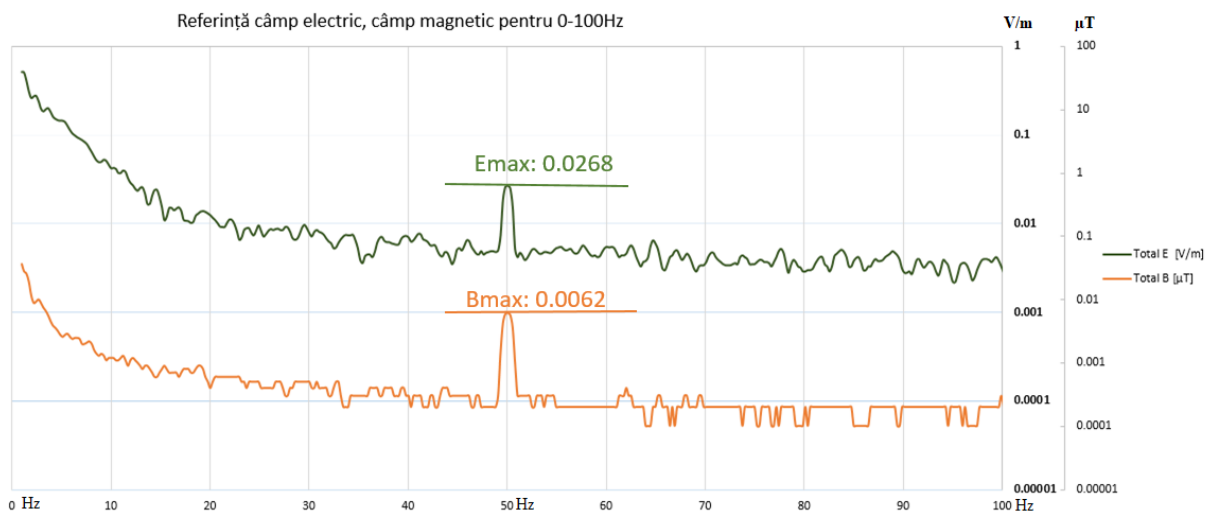


Figure 6.10: Magnetic and electric field representation – ambient noise reference measurement

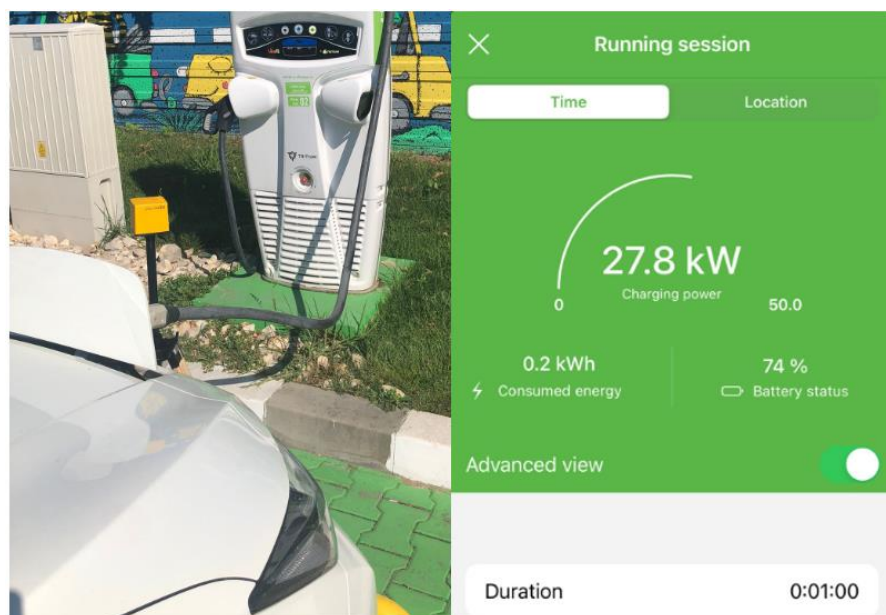


Figure 6.11: Actual measurement setup and charging parameters

In figure 6.11, you can see on the left the location of the car near the charging station, the location of the Narda EHP-50f antenna, and on the right we can see parameters during charging. The instantaneous charging power was 27.8 [kW] of the 50 [kW] maximum power supported by the charging station.

In this second set of measurements we will analyze the maximum values obtained at 50 [Hz] for the fast charging type, using the Chademo type connector.

In figure 6.12 I have represented the values of electric field strength and magnetic induction, with the antenna positioned near the car's charging connector.

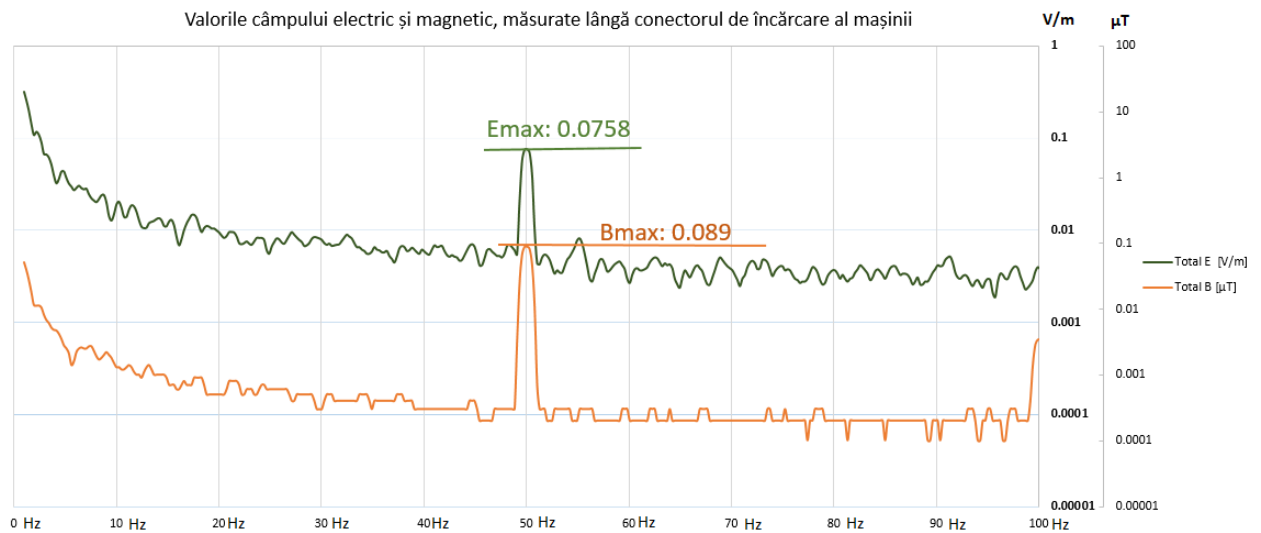


Figure 6.12: Representation of the magnetic and electric field in the frequency spectrum 0 – 100 Hz, for fast charging, the antenna positioned near the charging connector of the car

From the represented graph we can see that the maximum value obtained for the electric field intensity is 0.0758 [V/m], which is obtained at 50.05 [Hz]. The maximum value of the magnetic induction is also reached at the frequency of 50.05 [Hz] and has the value of 0.089 [μ T].

Comparing the values measured near the power connector with the ones imposed by ICNIRP 2010 (see Table 4.1), we can see that the electric field strength of 0.0758 [V/m] is lower than the limit imposed by the standard which is 5 [kV/m], as well as the magnetic induction value of 0.089 [μ T] is lower than the limit imposed by the standard which is 2×10^{-4} [T].

In figure 6.13 I represented the values of the electric field intensity and the magnetic induction, with the antenna positioned near the charging station.

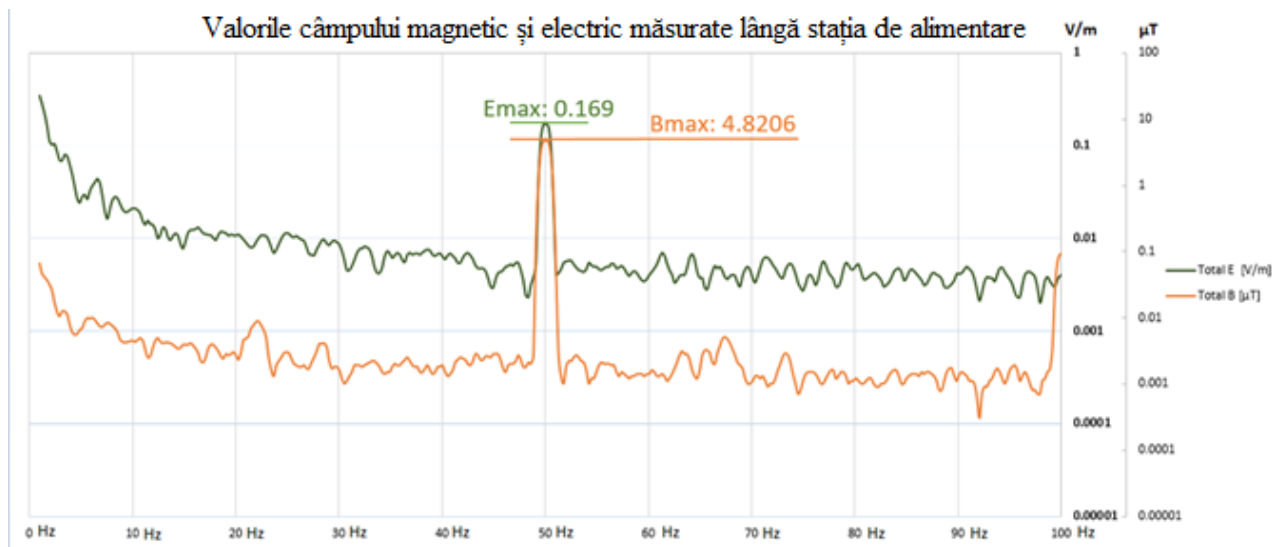


Figure 6.13: Representation of the magnetic and electric field in the frequency spectrum 0 – 100 Hz, for fast charging, the antenna positioned near the charging station

From the represented graph we can see that the maximum value obtained for the electric field intensity is 0.169 [V/m], the value obtained at 50.05 [Hz]. The maximum value of the magnetic induction is also reached at the frequency of 50.05 [Hz] and has the value of 4.8206 [μT].

Comparing the values measured near the charging station with the ones imposed by ICNIRP 2010 (see Table 4.1), we can see that the electric field intensity of 0.169 [V/m] is lower than the one imposed by the standard which is 5 [kV/m], as well as the magnetic induction value of 4.8206 [μT] is lower than the value imposed by the standard which is 2×10^{-4} [T].

Chapter 7: Electromagnetic field measurements of high voltage cables inside the body of electric vehicles

7.1. Installation used

Starting from the following sketch, the car housing was made on a 1: 2 scale.

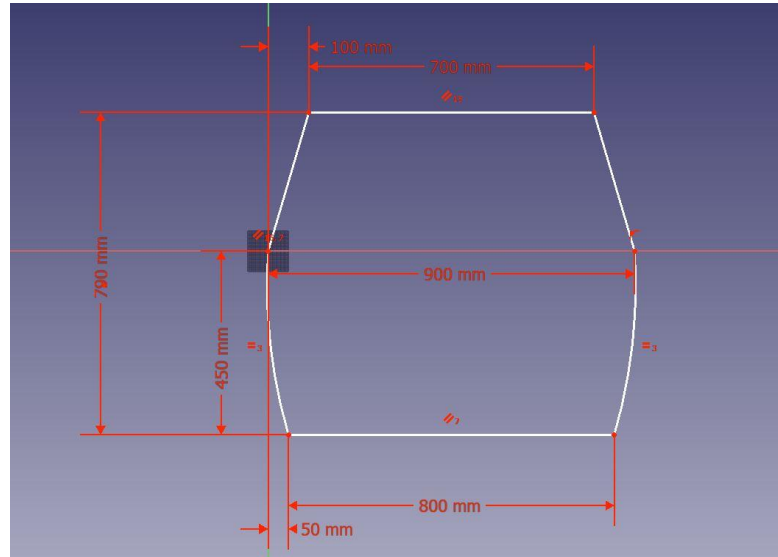


Figure 7.1: 1: 2 scale vehicle body diagram

Galvanized sheet with a thickness of 0.3 mm was used to make the housing. After handling it, it has the following structure:



Figure 7.2: 1: 2 scale vehicle body model

A 220 [V] to 6 [V] transformer was used to generate the current flowing through the cables to be positioned in the metal housing.

The secondary has been configured to achieve a current of 230A.

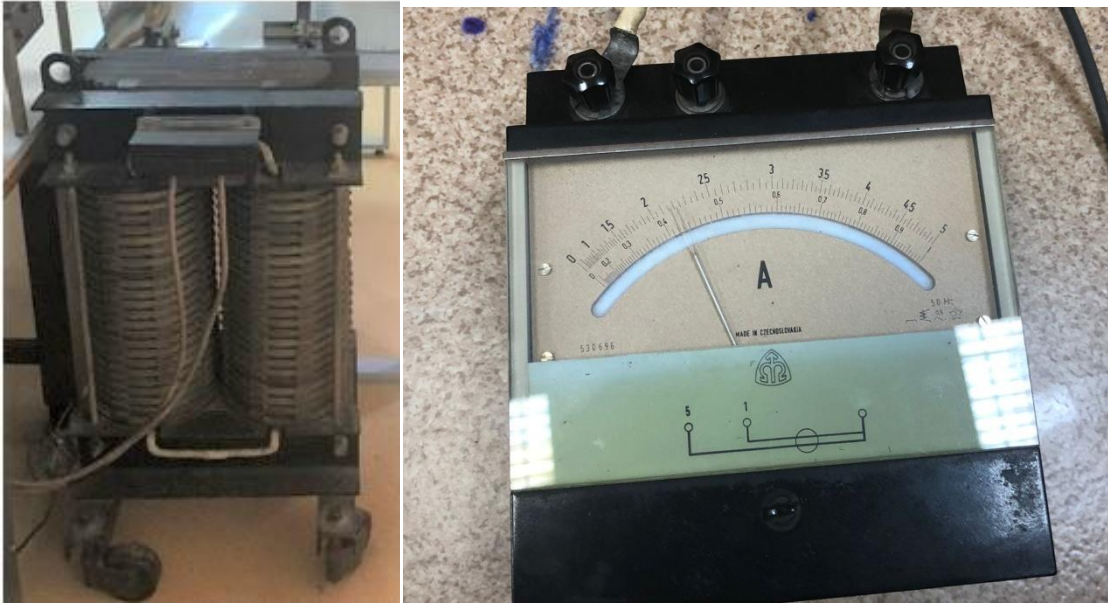


Figure 7.3: 220 [V] / 6 [V] Descending Transformer - Ammeter

A Gaussmeter 475 DSP was used to measure the magnetic field produced by the current flowing through the 2 cables inside the body:



Figure 7.4: Gaussmetru 475 DSP

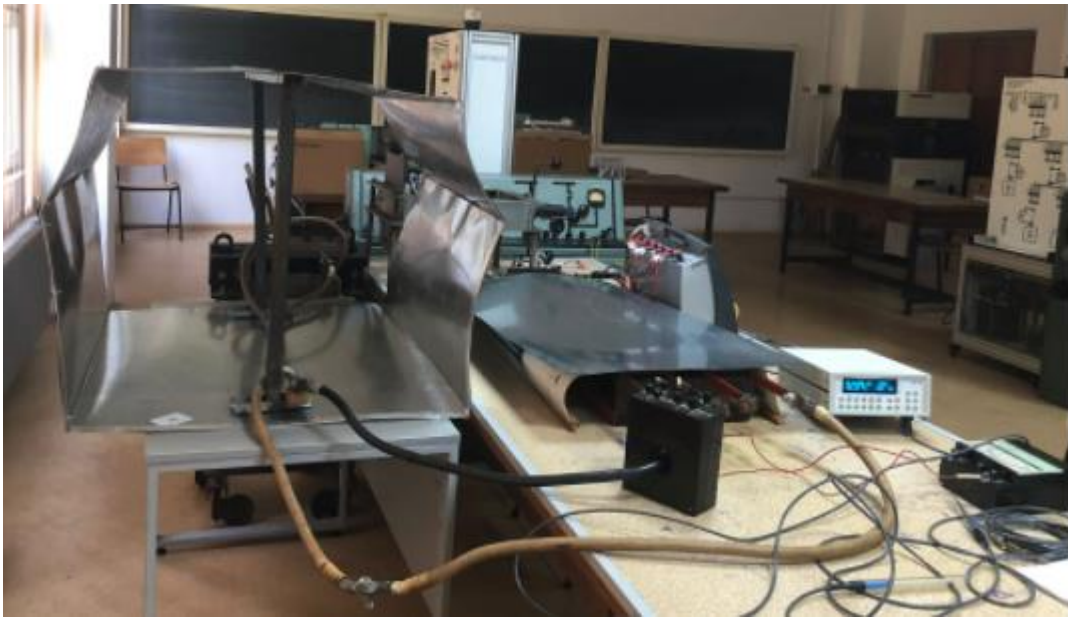


Figure 7.5: Experimental magnetic field measurement installation

The set of magnetic field experiments treats 4 distinct cases as follows.

7.2. Case 1: Both cables are positioned next to each other in the right corner of the body car

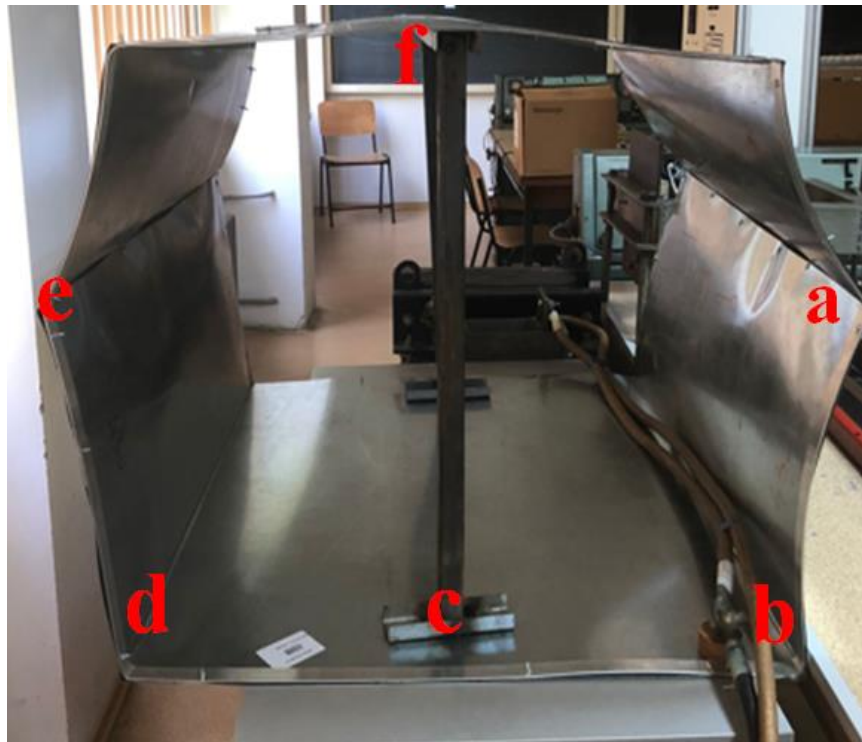


Figure 7.6: Both adjacent cables, positioned to the right of the body - the measuring points shown

Following the measurements made with the gaussmeter, using the perpendicular probe, the following values of the magnetic field were obtained:

	measured points					
Measuring points	a	b	c	d	e	f
Magnetic Field Measured Values	0.27	0.67	0.23	0.19	0.09	-

Table 7.1: Measured values of the magnetic field - case 1

In order to verify the accuracy of the measurements, with the help of the Femm program, the simulation of this case was performed.

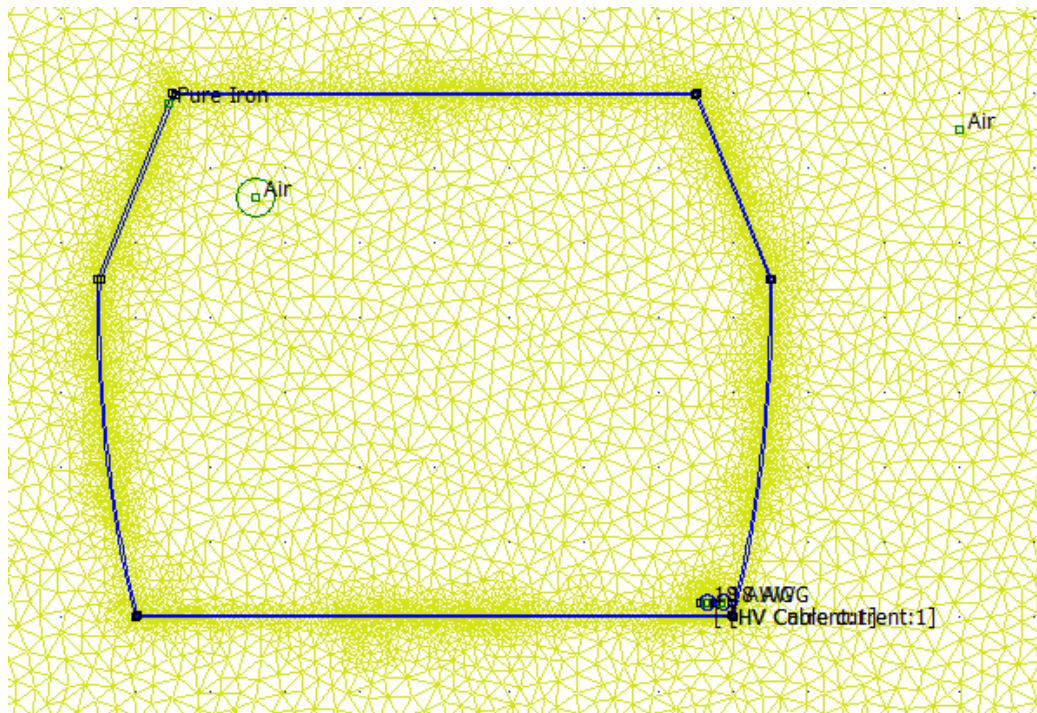


Figure 7.7: Simulation of case 1: both cables positioned in the right corner

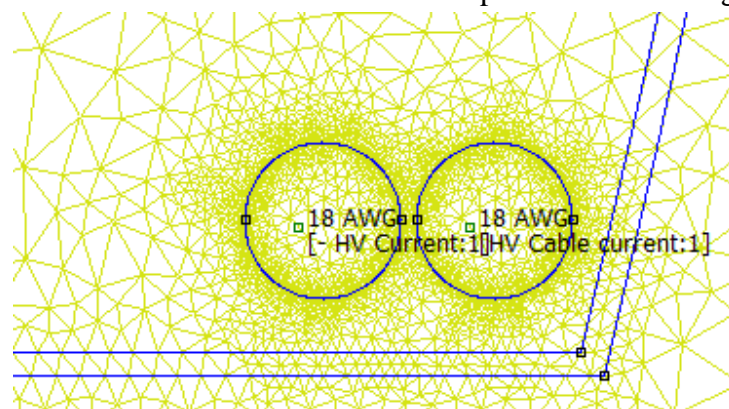


Figure 7.8: Cable arrangement

The 2 cables were assigned a circuit, in one of them the value of the assigned current is 230 [A], and in the other circuit the value of -230 [A], at the frequency of 0 [Hz].

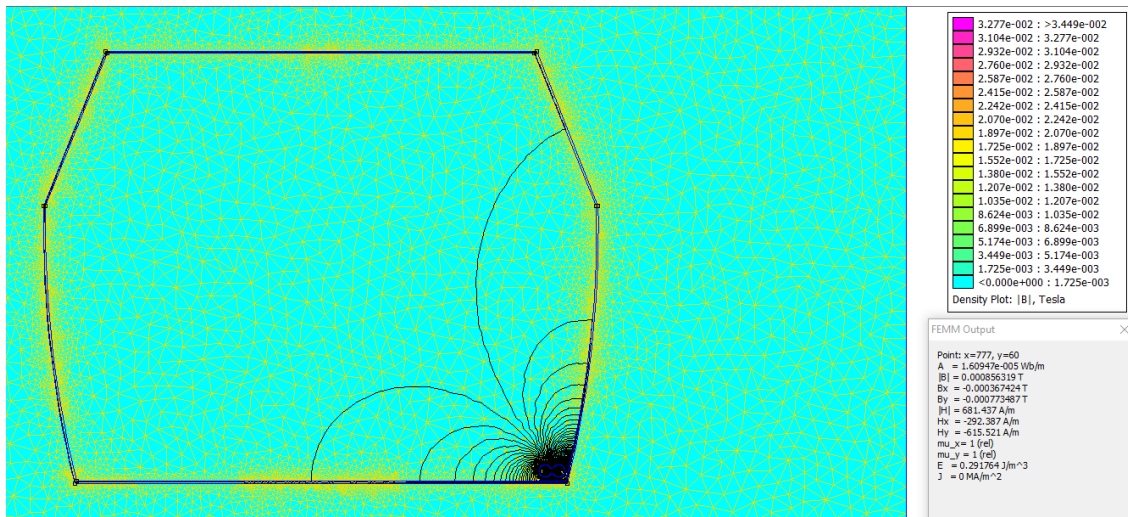


Figure 7.9: Distribution of magnetic field lines and value at the bottom right of the magnetic field

In the vicinity of the cables, the simulated value of the magnetic field is 0.85 [mT].

	measured points					
Measuring points	a	b	c	d	e	f
Simulated magnetic field values [mT]	0.29	0.85	0.3	0.1	0.063	-

Table 7.2: Simulated values of the magnetic field - case 1

Comparing the measured values with the simulated ones we obtain the following graph:

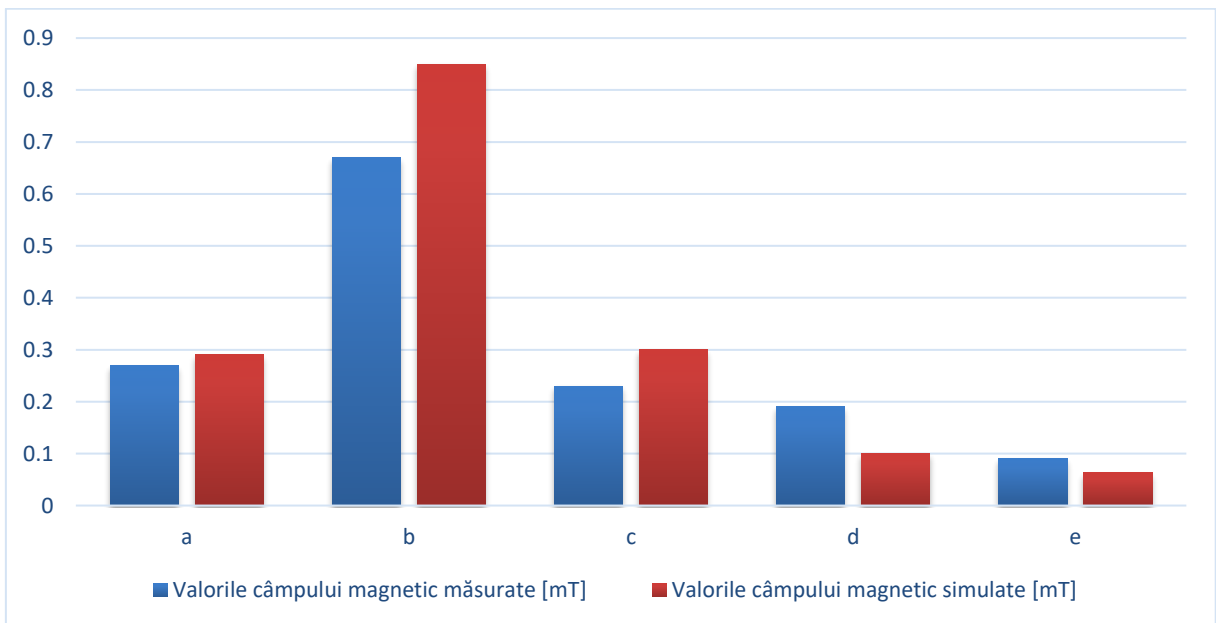


Figure 7.10: Measured versus simulated magnetic field values – case 1

7.3. Case 2: Both cables are positioned side by side in the center of the body car

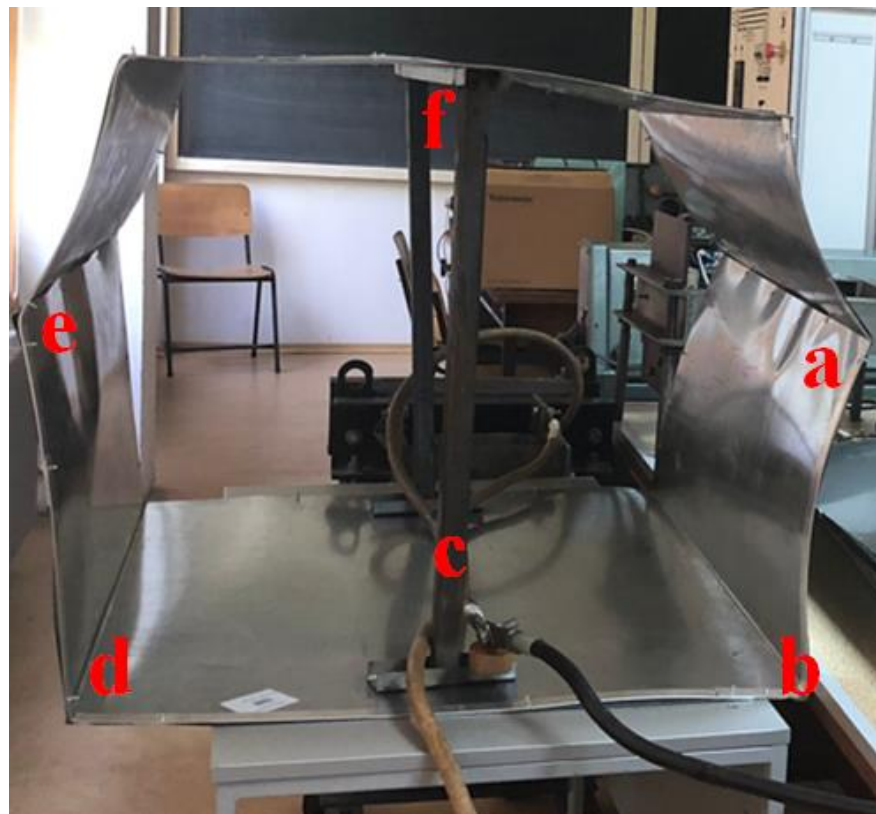


Figure 7.11: Both cables positioned in the center of the body

	measured points					
Measuring points	a	b	c	d	e	f
Magnetic field values mT	0.008	0.012	0.32	0.03	0.011	0.015

Table 7.3: Measured values of the magnetic field - case 2

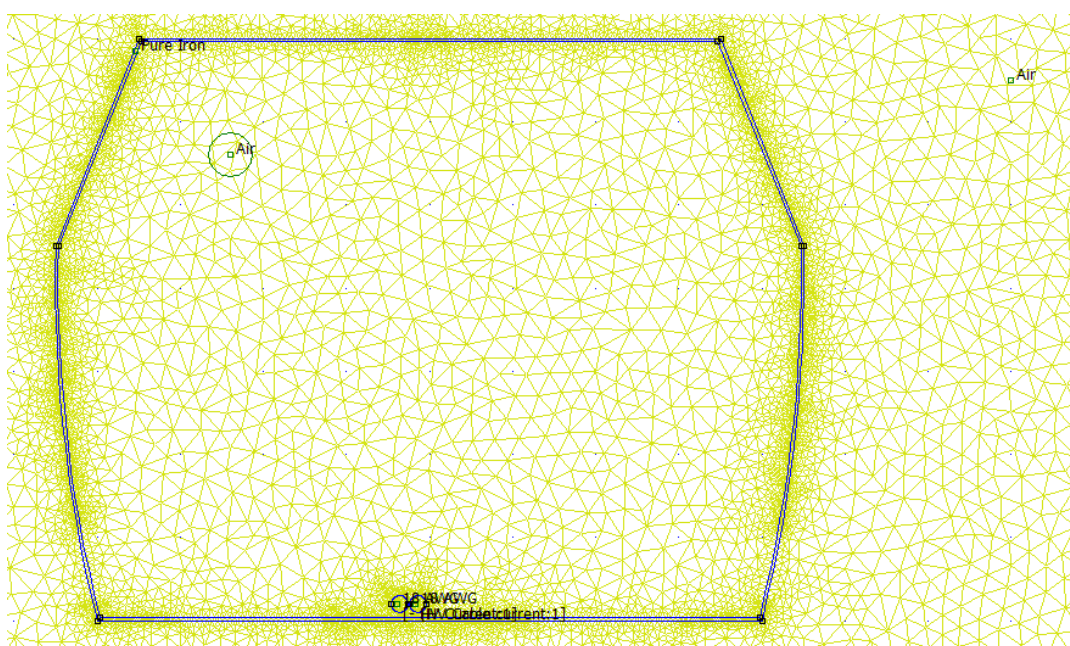


Figure 7.12: Simulation of case 2: both cables positioned centrally

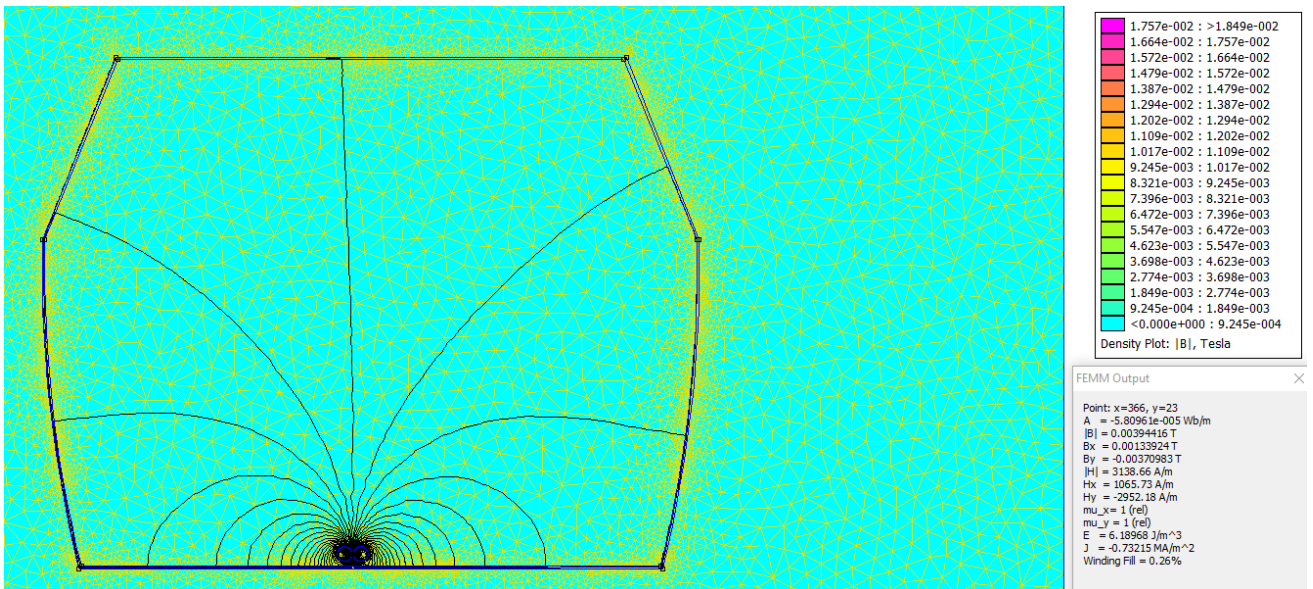


Figure 7.13: Distribution of magnetic field lines and value at the bottom center of the magnetic field

In the vicinity of the cables, the simulated value of the magnetic field is 0.39 mT.

	measured points					
Measuring points	a	b	c	d	e	f
Simulated magnetic field values [mT]	0.0057	0.019	0.39	0.02	0.007	0.008

Table 7.4: Simulated values of the magnetic field - case 2

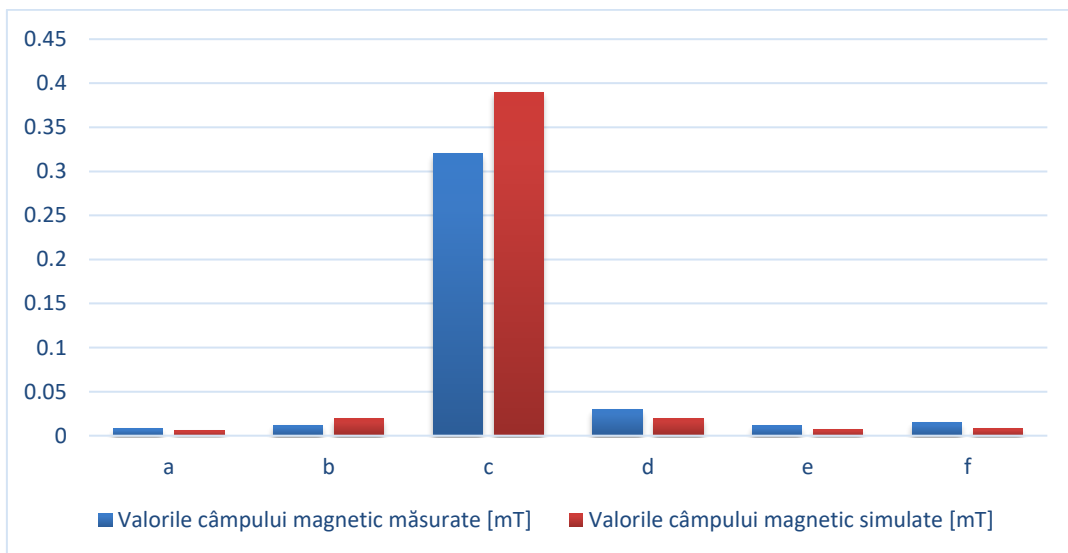


Figure 7.14: Measured versus simulated magnetic field values - case 2

7.4. Reverse cable - Symmetrical construction

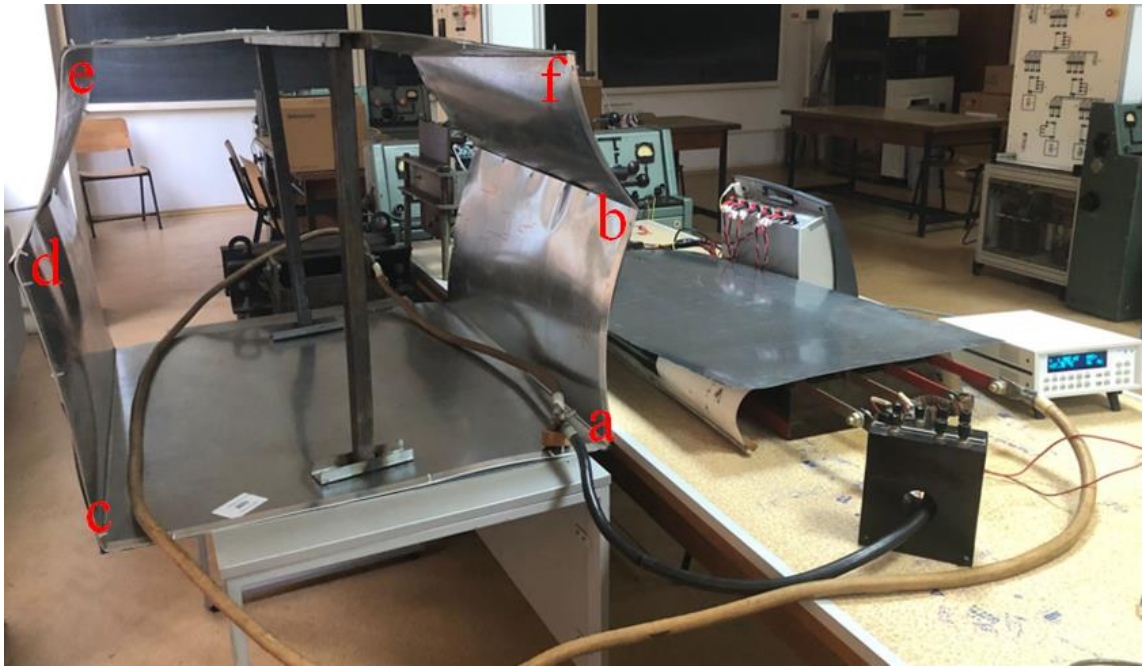


Figure 7.15: Cables laid in symmetrical construction

	Measured points					
	a	b	c	d	e	f
Measured magnetic field values [mT]	0.12	0.55	0.3	0.03	0.023	0.03

Table 7.5: Measured values of the magnetic field - case 3

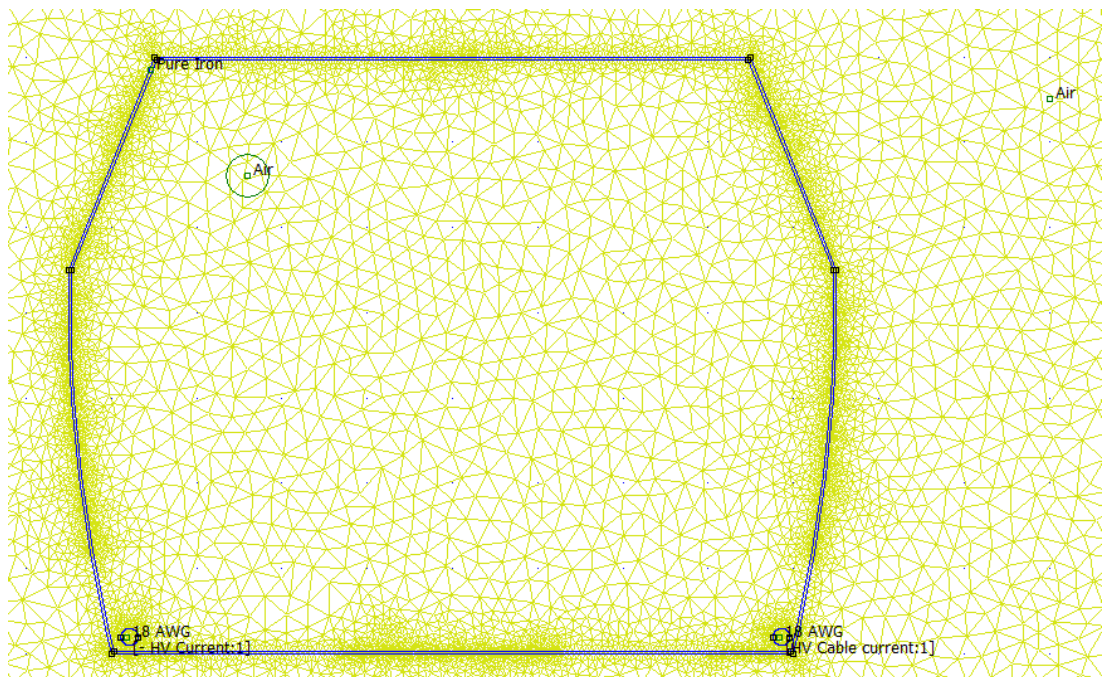


Figure 7.16: Mesh network - symmetrical construction

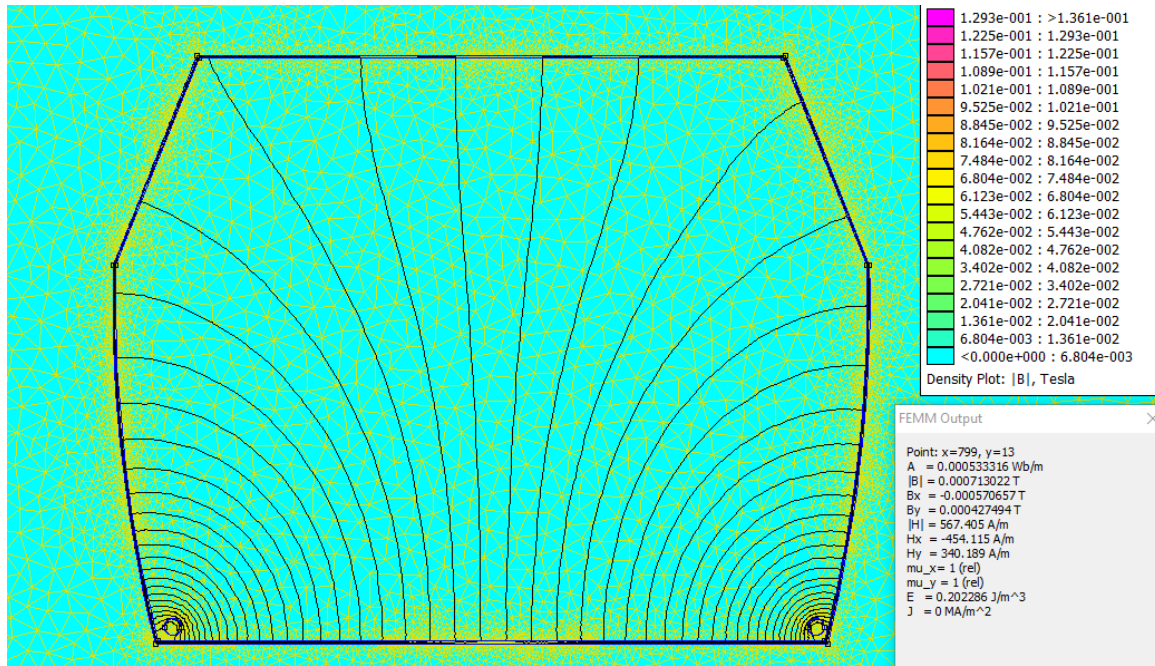


Figure 7.17: Distribution of magnetic field lines for symmetric construction and value at the bottom right of the magnetic field

	Measured points					
	a	b	c	d	e	f
Simulated magnetic field values [mT]	0.19	0.71	0.37	0.14	0.012	0.036

Table 7.6: Measured and simulated values of the magnetic field - symmetrical construction

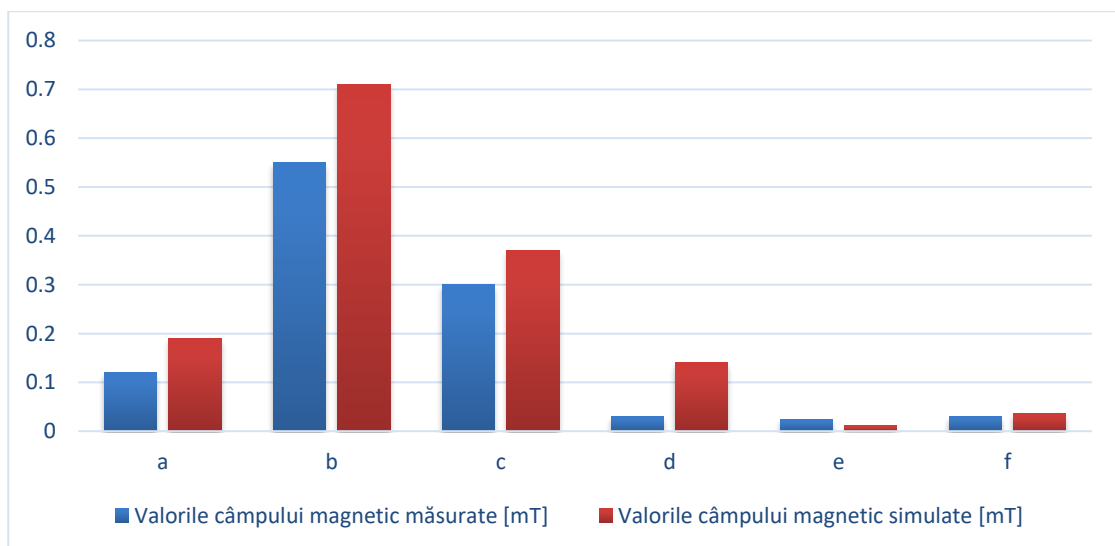


Figure 7.18: Measured versus simulated magnetic field values - case 3

7.5. Case 4: One cable is positioned to the right and one to the center

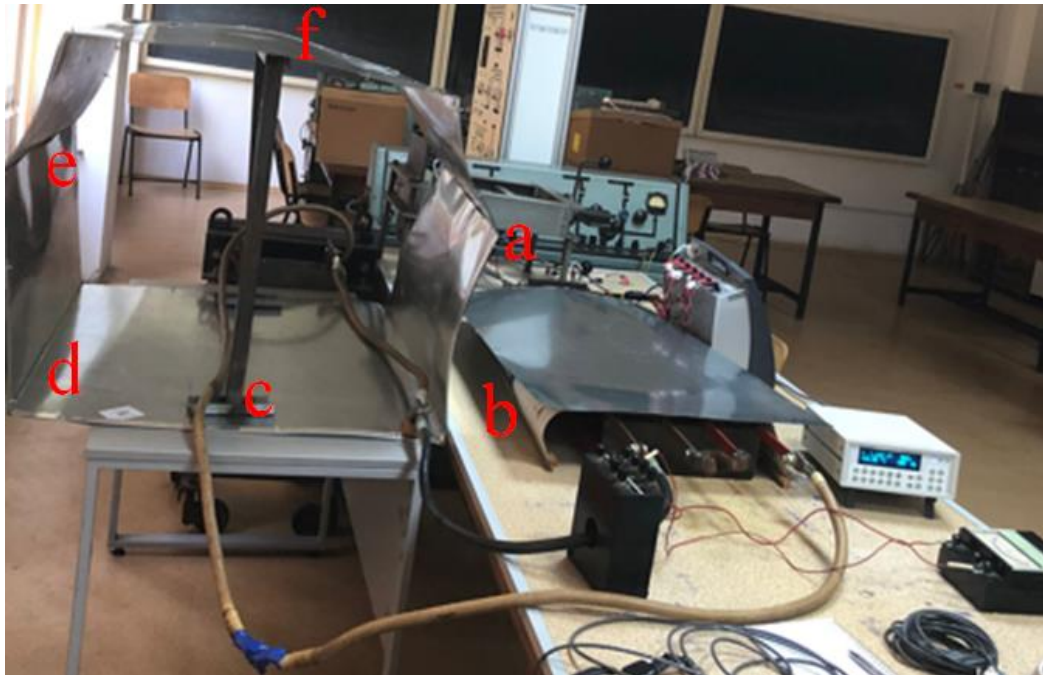


Figure 7.19: Cables laid in asymmetrical construction - one on the right and one on the center

	Punctele de măsură					
	a	b	c	d	e	f
Valorile câmpului magnetic măsurate [mT]	0.023	0.8	0.5	0.081	0.031	0.03

Table 7.7: Measured values of the magnetic field - case 4

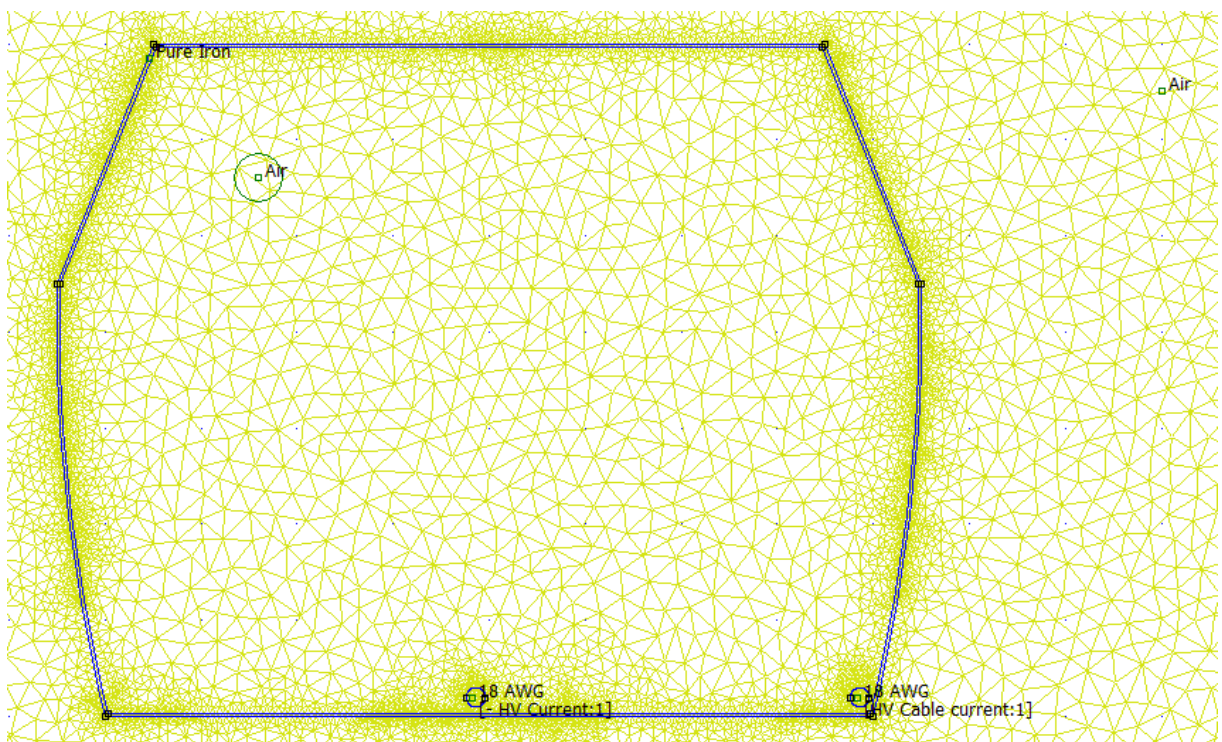


Figure 7.20: Mesh network - asymmetric construction

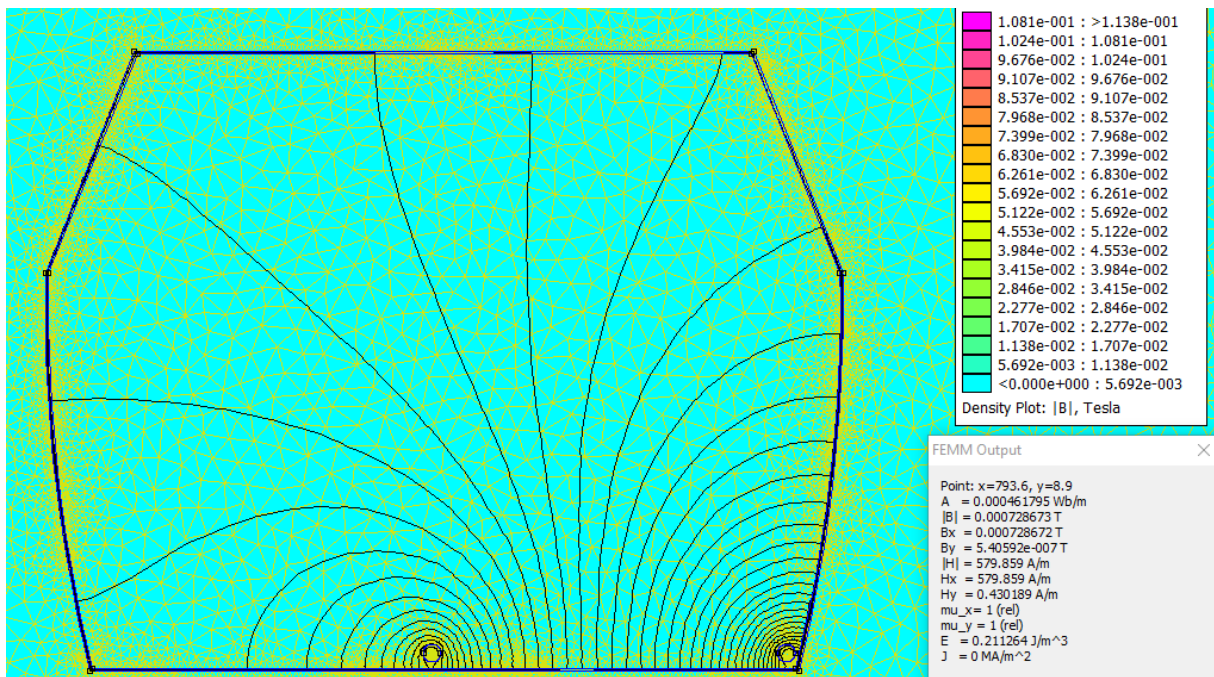


Figure 7.21: Distribution of magnetic field lines for asymmetric construction and value at the bottom right of the magnetic field

	Measured points					
	a	b	c	d	e	f
Simulated magnetic field values [mT]	0.12	0.72	0.7	0.006	0.045	0.092

Table 7.8: Measured and simulated values of the magnetic field - asymmetric construction

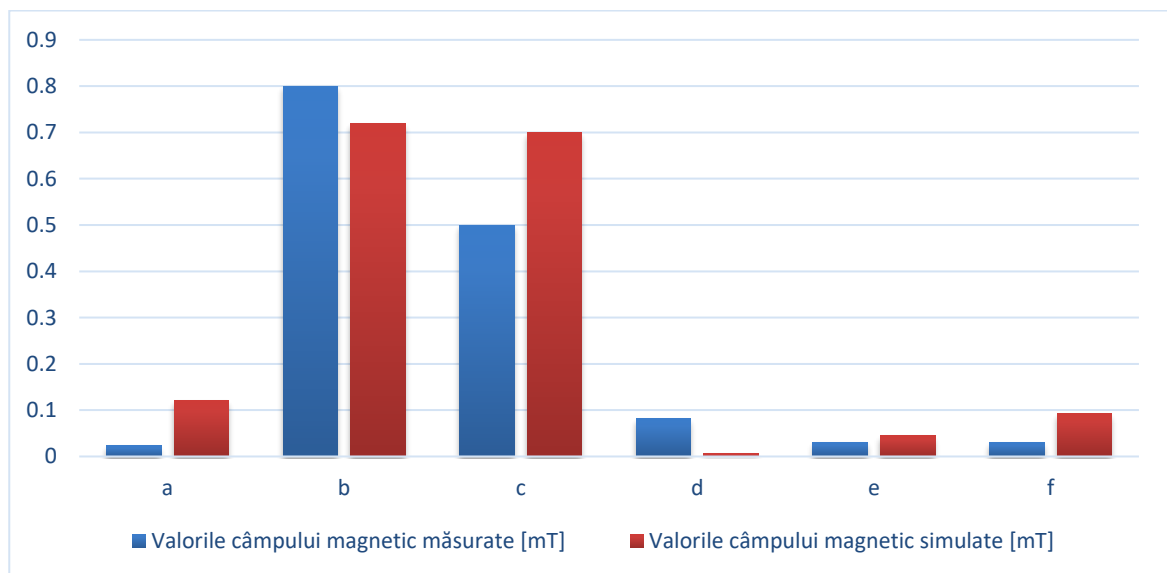


Figure 7.22: Measured versus simulated magnetic field values - case 4

Chapter 8: Conclusions and own contributions

8.1. General conclusions

This doctoral paper entitled "Electromagnetic Interference in Vehicle Electrical Systems" consists of 7 chapters.

The first chapter describes the basic concepts of electromagnetic compatibility, electromagnetic compatibility standards and a brief history of electric vehicles. The first battery-powered electric vehicle was built in 1834. 50 years after the advent of the electric vehicle, the first internal combustion engine was built in 1885. Electric vehicles were not as successful as combustion engines, which offered greater autonomy and were very easy to feed. In the latter part of the 20th century and the beginning of the 21st century, the electric vehicle began to regain ground in the automotive industry due to new regulations related to environmental protection and due to the development and improvement of the construction of rechargeable batteries, engine and controllers.

Chapter 2 presents the 3 main construction structures of electric and hybrid vehicles: the electric battery vehicle, the hybrid electric vehicle and the plug-in hybrid vehicle, highlighting the components of each and the differences between them.

The third chapter identifies and analyzes significant field sources in electric vehicles. The main elements of the new electric vehicle drive systems are the electric motor, the static power converter, the power supply and the connecting lines. Each component of the drive system creates a transfer path for electromagnetic interference. The power converter is the main source of electromagnetic interference. The components of the drive system were analyzed as either a source of electromagnetic noise or part of the coupling mechanism.

In the fourth chapter, the prevention regulations and standards were briefly presented: the ICNIRP regulations and the IEEE standard. Possible victims of electromagnetic interference have been reported. In the case of electric vehicles, passengers are very close to electrical systems that have significant power, usually for considerable periods of time. The relatively high currents reached by these systems and the short distances between power devices and

There are mainly 3 organizations that write and maintain regulations in the automotive field: CISPR, ISO and SAE. As there are many other areas of interest for EMC, there are many government organizations that also regulate component testing. In most cases, these standards are based on CISPR and ISO documents to guide the test and the optimal test environment.

Today's cars are equipped with many more electronic devices, ADAS devices which means more sensors, high speed systems, complex radar wiring and yet all systems need to operate in optimal parameters, without errors and without interfere with other systems in the vehicle.

In order for the vehicle systems and the vehicle as a whole not to emit electromagnetic disturbances and not to be susceptible to disturbances, the regulations in the field of automotive electromagnetic compatibility must be analyzed.

Every car manufacturer has formulated its own internal standards that specify the levels and test methods that the components used in their vehicles must meet. These internal regulations are also based on CISPR and ISO documents. American car manufacturers use SAE documents. [13]

Chapter 5 shows the simulation of the magnetic field produced by the high voltage cable that connects the intelligent battery system to the electric motor in seven different topologies. These magnetic simulations were performed using the FEMM program. In 6 of the simulated cases the Copper conductor was used, so that in the 7th case the coaxial cable was used, observing how the magnetic field lines close inside it.

Analyzing and comparing the maximum values obtained for magnetic induction in each case we can extract the lowest maximum value, with the value of 0.1195 [T] obtained for the second case: round trip cable path - symmetrical construction and the highest maximum value of magnetic induction of 0.295 [T] obtained for the 4th case: cable path with return through the housing - symmetrical construction - 0 cm from the floor.

It is important to note that these maximum magnetic induction values for each case are obtained either inside the coaxial cable or inside the vehicle body. In areas where the passenger is exposed, these values are much lower, for example near the windows a value of 0.5 [μ T] is obtained.

By comparing the results of the simulations with the 2010 ICNIRP regulation, it can be concluded that the values obtained in the 7 cases are lower than the regulated reference level for the general public, which is 400 [mT].

In Chapter 6 we studied the interaction between the surrounding electromagnetic environment and the electric vehicle. The introduction of BEVs in public transport will raise some issues of electromagnetic compatibility. Also here I have measured the electric and magnetic field during the slow and fast charging process.

Chapter 7 deals with magnetic field measurements made inside a galvanized sheet metal housing for 2 cables connected to a transformer that supplies them at 230 [A]. 4 distinct cases were treated for different topologies. In order to verify the correctness of the laboratory measurements, magnetic field simulations were performed, finally comparing the measured values with the simulated ones.

8.2. Personal contributions

The paper presents the following original contributions:

- Simulation of the magnetic field produced by the high voltage cable inside the electric vehicle in different topologies:
 - Cable path with return through the housing - asymmetrical construction
 - Round trip cable route - Symmetrical construction
 - Cable path with return through the housing - symmetrical construction
 - Cable path with return through the housing - symmetrical construction - 0 cm from the floor
 - Cable path with return through the housing - symmetrical construction - 10 cm from the floor
 - Cable track with return through the housing - symmetrical construction - 10 cm from the floor with seats
 - Coaxial cable magnetic field simulation - asymmetric construction

- Study of the interaction between the surrounding electromagnetic environment and the electric vehicle:
 - Analysis and simulation of the ambient electromagnetic environment outside the electric vehicle being analyzed the magnetic field produced by a medium voltage line
 - Simulation of the magnetic field produced by a medium voltage energy transfer line in the presence of a body
 - Analysis of the ambient electromagnetic environment inside the passenger compartment of the electric vehicle
 - Electric and magnetic field measurement during charging of an electric vehicle with Type2 connector – slow charging
 - Electric and magnetic field measurement during charging of an electric vehicle with Chademo type connector – fast charging

- Experiments on the magnetic field produced by high voltage cables inside the body of electric vehicles for different topologies:
 - Both cables are positioned next to each other in the right corner of the body
 - Both cables are positioned next to each other in the center of the body
 - Round cable - Symmetrical construction
 - One cable is positioned to the right and one to the center

- Magnetic field simulations produced by high voltage cables inside the body of electric vehicles for different topologies:
 - Both cables are positioned next to each other in the right corner of the body
 - Both cables are positioned next to each other in the center of the body
 - Round cable - Symmetrical construction
 - One cable is positioned to the right and one to the center

- Comparing the results obtained from laboratory experiments with those obtained from simulations.

8.3. Future directions of research

For the future, the following could be analyzed and developed:

- Magnetic field measurement in various types of electric, hybrid and conventional vehicles in all operating modes
- Magnetic field analysis in plastic carcass structures
- Comparison between aluminum and plastic carcass structures from an electromagnetic point of view.

List of published articles

1. **Violeta-Maria IONESCU**, Anca-Alexandra SĂPUNARU, Claudia Laurența POPESCU, Mihai Octavian POPESCU, “EMC Normes for Testing Electric and Hybrid Cars” (EV2019) (PoD) ISBN:978-1-7281-0792-9, Electronic ISBN:978-1-7281-0791-2, DOI: 10.1109/EV.2019.8892881
2. Anca-Alexandra SĂPUNARU, **Violeta-Maria IONESCU**, Mihai Octavian POPESCU, Claudia Laurența POPESCU, “Study Of Radiated Emissions Produced By An Electric Vehicle In Different Operating Modes” (EV2019) (PoD) ISBN:978-1-7281-0792-9, Electronic ISBN:978-1-7281-0791-2, DOI: 10.1109/EV.2019.8893142
3. **Violeta-Maria IONESCU**, Anca-Alexandra SĂPUNARU, Mihai Octavian POPESCU, Claudia Laurența POPESCU, “Magnetic Field Constraints in the Passenger Compartment of Electric Vehicles” (ISGT-Europe) (PoD) ISBN:978-1-5386-8219-7, Electronic ISBN: 978-1-5386-8218-0, DOI: 10.1109/ISGTEurope.2019.8905554
4. Anca-Alexandra SĂPUNARU, **Violeta-Maria IONESCU**, Mihai Octavian POPESCU, Claudia Laurența POPESCU, “Propagation Phenomena of Conducted Disturbances in a Converter Powered through a LISN” (ISGT-Europe) (PoD) ISBN: 978-1-5386-8219-7, Electronic ISBN: 978-1-5386-8218-0, DOI: 10.1109/ISGTEurope.2019.8905620
5. **Violeta-Maria IONESCU**, Anca-Alexandra SĂPUNARU, Mădălina-Andreea LUPAȘCU, Mihai Octavian POPESCU, Claudia Laurența POPESCU, “Electromagnetic Interaction between the Power Distribution Grid and the Hv System of an Electric Vehicle” (Foren 2020); Journal title: EMERG - Energy.Environment. Efficiency. Resources. Globalization ISSN: 2457-5011 (print), 2668-7003 (online) EMERG 2020; 6 (3) : 77-84; 10.37410/EMERG.2020.3.07
6. Anca-Alexandra SĂPUNARU, **Violeta-Maria IONESCU**, Ovidiu FRĂȚILĂ, Mădălina Andreea LUPAȘCU, Mihai Octavian POPESCU, Claudia Laurența POPESCU, “Active Power Transfer between two Energetic Networks, of Different Working Frequencies, using a Variable Frequency Transformer” (Foren 2020)
Journal title: EMERG - Energy.Environment. Efficiency.Resources.Globalization ISSN 2457-5011 (print), 2668-7003 (online) EMERG 2/2021; Vol. 7, Issue 2, pp. 48-54 (2021), DOI: 10.37410/EMERG.2021.2.04
7. Andreea - Mădălina LUPAȘCU, **Violeta-Maria IONESCU**, Ion POTĂRNICHE, Valentin NĂVRĂPESCU , Anca-Alexandra SĂPUNARU, “Increase of Energy Efficiency of Electrically Driven Drilling Installations by Valorising the Braking Regime of The Draw Works upon Descending the Pipe Line”, (Foren 2020).
Journal title: EMERG - Energy.Environment. Efficiency.Resources.Globalization ISSN: 2457-5011 (print), 2668-7003 (online) Publisher: AGIR F EMERG 2020; 6 (3): 33-40; 10.37410/EMERG.2020.3.03

Bibliography

- [1] James Larminie, John Lowry – „Electric Vehicle Technology Explained”, John Wiley & Sons Ltd, 2003
- [2] Mark Steffka – „Automotive EMC Introduction and Overview”, University of Michigan - Dearborn
- [3] Gary Fenical – „A Primer on Automotive EMC for Non-EMC Engineers”, 2013
- [4] C. C. Chan - „The rise & fall of electric vehicle in 1828-1930: Lessons learned”, Proceedings of the IEEE, 2013
- [5] https://www.afdc.energy.gov/vehicles/electric_basics_ev.html, 16.05.2018
- [6] Ramesh C. Bansal - „Handbook of automotive power electronics and motor drives”, Taylor & Francis Group, LLC, 2005
- [7] Monzer Al Sakka, Joeri Van Mierlo, Hamid Gualous – “DC/DC Converters for Electric Vehicles”, Intech, 2011
- [8] S. Guttowski, S. Weber, E. Hoene, W. John, H. Reichl – “EMI in Electric Vehicles”, 2014
- [9] Pablo Moreno-Torres, Marcos Lafoz, Marcos Blanco, Jaime Arribas – “Passenger Exposure to Magnetic Fields in Electric Vehicles”, Intech, 2016
- [10] Maurizio di Paolo Emilio – „Automotive EMC”, Interference Technology guide series, 2018
- [11] Kenneth Wyatt – „Basic EMI Concepts”, Interference Technology guide series, 2018
- [12] Kal Mustafa – „Design and Layout Guidelines for the CDCVF2505 Clock Driver”, Texas Instruments, 2000
- [13] Vicente Rodrigues – “Automotive Component EMC Testing: CISPR 25, ISO 11452-2 and Equivalent Standards”, SAFETY & EMC, 2011
- [14] Todd Hubing – “Common Commercial, Automotive, Medical, Wireless & Military EMC standards”, Interference Technology guide series, 2018
- [15] Online:https://www.com-power.com/ah220_horn_antenna.html, 01.12.2018
- [16] Eduard Luncă – “Compatibilitate electromagnetică – Teste și măsurări specifice”, Editura Pim, Iași, 2015
- [17] Timothy Hegarty - “An overview of radiated EMI specifications for power supplies”, Texas Instrument, June 2018
- [18] Garth D’Abreu, Craig Fanning, Ammar Sarwar - “EMC Standards and Chamber Testing for Automotive Components”, InCompliance, February 2016
- [19] Enoch Eapen, Aditi Sethi - “Electric Vehicle - EMC aspects”, Icat, April 2018

- [20] Violeta-Maria Ionescu, Anca-Alexandra Săpunaru, Mihai Octavian Popescu, Claudia-Laurența Popescu - "EMC Normes For Testing Electric And Hybrid Cars", EV2019
- [21] Linda Dawson, Andrew Dawson, Alastair Ruddle, Lester Low, Rob Armstrong, "EMC Measurements and testing for FEVs," *Electrical powertrain health monitoring for increased safety of FEVs*, pp. 4-8, 25 March 2014.
- [22] Pablo Moreno-Torres, MarcosLafoz, Marcos Blanco, Jaime R. Arribas, "Passenger exposure to magnetic fields in electric vehicles," *INTECH*, pp. 47-52, 2016.
- [23] Andrea Vassilev, Alain Ferber, Christof Jan Wehermann, Olivier Pinaud, Meinhard Schilling, Alastair R. Ruddle, "Magnetic field exposure assessment in electric vehicles", *IEEE transactions on electromagnetic compatibility*, pp. 1-2, February 2015.
- [24] Martin März, Andreas Schletz, Bernd Eckardt, Sven Egelkraut, Hubert Rauh, "Power electronics system integration for electric and hybrid vehicles", *IEEE Xplore*, pp. 1-2, March 2010.
- [25] David Meeker, "Finite Element Method Magnetics", pp. 6-7, October 25, 2015. [Online]: <http://www.femm.info/Archives/doc/manual.pdf>
- [26] ICNIRP 2010: International Commission on non-ionizing Radiation Protection, ICNIRP statements-Guidelines for limiting exposure to time-varying electric and Magnetic fields (1 Hz to 100 kHz), *Health Physics* 99 (6), page 818-836, 2010
- [27] ICNIRP Publication, 2009. ICNIRP Guidelines on limits of exposure to static magnetic fields. *Health Physics* 96(4):504-514; 2009, pages: 510-512. [Online]. Available <https://www.icnirp.org/cms/upload/publications/ICNIRPstatgdl.pdf>
- [28] [Online]: <https://en.wikipedia.org/wiki/Electromagnetism>
- [29] [Online]: https://en.wikipedia.org/wiki/Electromagnetic_spectrum
- [30] Violeta-Maria Ionescu, Anca-Alexandra Săpunaru, Mihai Octavian Popescu, Claudia Laurența Popescu - „Magnetic Field Constraints in the Passenger Compartment of Electric Vehicles”, 2019 IEEE PES Innovative Smart Grid Technologies Europe (ISGT-Europe)
- [31] Violeta-Maria Ionescu, Anca-Alexandra Săpunaru, Mădălina-Andreea Lupașcu, Mihai Octavian Popescu, Claudia Laurența Popescu – „Electromagnetic Interaction between the power distribution grid and THE HV system of an electric vehicle”, FOREN2020
- [32] Popescu M.O. – Compatibilitate electromagnetică, Aplicații la Convertoare statice de putere;
- [33] Hortopan Gheorghe – Principii și tehnici de compatibilitate electromagnetică – ET Buc 2005;
- [34] Schwab A. – Compatibilitate electromagnetică, ET, București 1996 (Traducere in română);
- [35] Popescu Claudia s.a, CEM – Sinteze si aplicatii, Ed.Ars Docendi Bucuresti 2004;
- [36] http://telecom.etc.tuiasi.ro/telecom/staff/vlcehan/discipline%20predate/cem/%281%29%20CEM_introducere.pdf;
- [37] http://www.sier.ro/Articolul_6_1_2.pdf.